



The role of gateways in the evolution of temperature and salinity of semi-enclosed basins: An oceanic box model for the Miocene Mediterranean Sea and Paratethys

M.P. Karami^{*}, A. de Leeuw, W. Krijgsman, P.Th. Meijer, M.J.R. Wortel

Department of Earth Sciences, Faculty of Geosciences, Utrecht University, Utrecht, Netherlands

ARTICLE INFO

Article history:

Received 10 December 2010

Accepted 26 July 2011

Available online xxx

Keywords:

box model
gateway closure
semi-enclosed sea
Paratethys
Miocene
Mediterranean Sea

ABSTRACT

Marine gateways are important for semi-enclosed basins as they control exchange flows and influence water circulation. During much of the Early and Middle Miocene (~23–13 Ma), the Paratethys (of which at present only the Black Sea and Caspian Sea remain) and the Mediterranean Sea were connected to both the Atlantic and Indian Oceans. The gateways to the Indian Ocean were closed ultimately in the Middle Miocene. Here, we apply an oceanic 4-box model to determine the temperature, salinity and exchange flows for the Paratethys and the Mediterranean Sea before and after closure of the Indian Ocean gateways. Our analysis forms a novel way of linking tectonics, climate and basin evolution. We investigate whether changes observed in the geological record of Paratethys are caused by changes in gateway configuration or in climate. We mainly focus on Paratethys which, because of the availability of a large variety of geological studies, presents an outstanding opportunity for studying the evolution of semi-enclosed basins and the impact of gateway closure. Moreover, Paratethys is considered to have played an important role in the evolution of Eurasian climate. Our analysis explores various values of the model parameters such as net evaporation and surface heat flux. Our main conclusions are: (1) Paratethys became more responsive to climate change after closure, (2) closure of the gateways to the Indian Ocean probably caused cooling of Paratethys and, in particular, accounted for the enigmatic Mid-Burdigalian cooling in Paratethys, (3) closure induced a change in salinity of Paratethys which is dependent on the net evaporation and size of the gateway connecting Paratethys to the Mediterranean, (4) Paratethys is sensitive to closure of both the gateway between Paratethys and the Indian Ocean, and the gateway between the Mediterranean Sea and the Indian Ocean, (5) Paratethys is influenced by the water properties of the Mediterranean Sea, (6) the water properties of Paratethys have only very limited influence on the Mediterranean Sea, and (7) in the advanced stage of the closure, the Mediterranean/Paratethyan temperature and salinity became more responsive to the restriction of the eastern gateways.

© 2011 Elsevier B.V. All rights reserved.

1. Introduction

Marine gateways play a crucial role in the exchange of water, heat and salt between ocean basins. Tectonically induced changes in gateway geometry can alter ocean circulation and heat transport, which in turn can cause climate change on a regional scale and potentially on the global scale (e.g., Hay, 1996). For instance, model results of Omta and Dijkstra (2003) indicated that constriction of the Tethys Seaway in combination with the widening of Drake Passage reversed the exchange flow through the Panama Seaway in the Early Miocene (~23 Ma). This has been suggested to result in cooling of the Caribbean surface waters and may have caused the demise of warm-water corals (von der Heydt and Dijkstra, 2005). In another example, the emergence of the Isthmus of Panama at around 4.6 Ma is thought to have intensified the Gulf Stream and transported warm and saline

water to high northern latitudes (Haug and Tiedemann, 1998; Bartoli et al., 2005).

For enclosed or semi-enclosed basins, marine gateways are even more important because they are the only means of communication with other basins. The opening or disruption of gateways, resulting from tectonic activity and/or sea level variations, may significantly change the temperature, salinity and sedimentary environment of the semi-enclosed basin (e.g., recently, Alhammoud et al., 2010; Thompson et al., 2010). Located in the convergence zone between Africa and Eurasia, the Mediterranean Sea and Paratethys had gateways to both the Atlantic and the Indian Oceans during much of the Early and Middle Miocene (~23–13 Ma; Fig. 1). The gateways to the Indian Ocean were closed sometime in the Middle Miocene (Rögl, 1999; Meulenkamp and Sissingh, 2003; Reuter et al., 2009). The geological record suggests that disconnection from the Indian Ocean led to severe changes in the water properties of both the Mediterranean and Paratethys (Rögl, 1999; Latal et al., 2004; Harzhauser et al., 2007b). In Paratethys, intermittent gateway disruption, in combination with sea level variations, caused major turnovers in the composition of flora and fauna (Harzhauser et al.,

^{*} Corresponding author.

E-mail address: karami@geo.uu.nl (M.P. Karami).

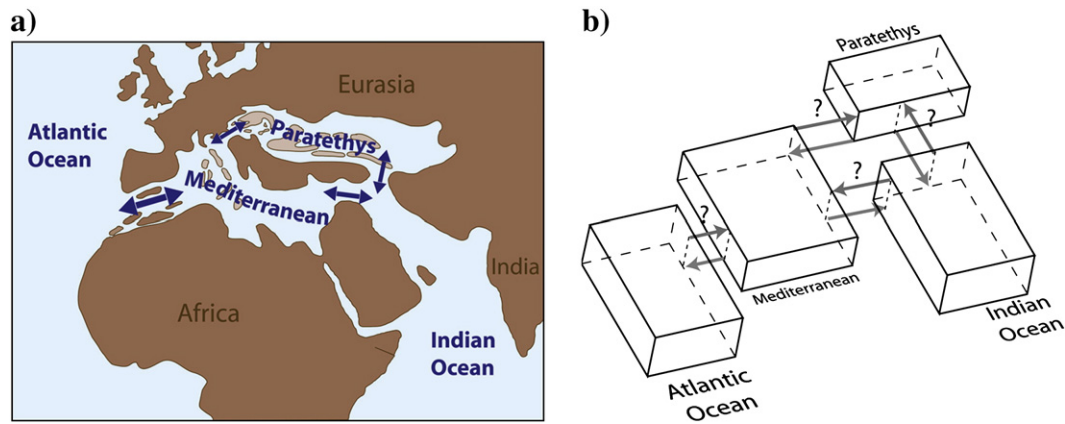


Fig. 1. a) Sketch of the paleogeography of the Early to Middle Miocene Mediterranean Sea and Paratethys prior to closure of their connections to the Indian Ocean (after Rögl, 1999). b) Cartoon of corresponding 4-box model with arrows showing the exchange flows. Question marks are indicating that exchange flows are not known.

2002; 2007a). However, the cooling and warming trends in the geological record of Paratethys and the Mediterranean, inferred from changes in faunal assemblages or shifts in oxygen isotope values, are often interpreted as a reflection of changes in global or local climate (e.g., Kocsis et al., 2008). It is of much interest to understand to what extent these changes observed in proxy data are actually controlled by changes in the gateways.

The purpose of this study is to investigate the gateway control on the Paratethyan temperature and salinity by using an ocean model. The model offers a new means to address the complex interplay of tectonic and climatic factors in basin evolution. The availability of detailed proxy records makes Paratethys a very suitable case for studying the evolution of semi-enclosed basins. The evolution of Paratethys deserves to be understood in detail also because the sea is considered an important player in the development of Eurasian climate (Ramstein et al., 1997; Zhang et al., 2007).

The only previous model study concerning the effects of closure of the gateway to the Indian Ocean is our oceanic 3-box model (Karami et al., 2009) in which Paratethys is considered a part of the Mediterranean Sea and is not represented as a separate basin. Although the use of a 3-box model is valid as a first step, a separate box representing Paratethys is needed in order to address the possibility of different atmospheric forcing over the Mediterranean and Paratethys. Also, this allows us to examine the scenario in which the Mediterranean Sea is disconnected from the Indian Ocean while Paratethyan–Indian connection remains open or vice versa (e.g., early Serravallian reconstruction of Rögl, 1998).

We thus apply an oceanic 4-box model to achieve quantitative insight into the effect of gateways, and especially their closure, on the water properties of Paratethys and the Mediterranean Sea. We also aim to determine possible configurations of the exchange flows. Theoretical predictions of the new 4-box model are compared with isotope data and inferences based on biota in order to understand better the factors that controlled the evolution of the sedimentary record of Paratethys. Our findings also include new results concerning the Mediterranean Sea resulting from the fact that it is now considered separate from Paratethys (cf. Karami et al., 2009). This study is to contribute to the general understanding of the role of gateways in determining water properties and circulation of land-locked basins.

2. Model description

2.1. Basin configuration

By the end of the Eocene (~34 Ma), the northward drift of Africa and several other Gondwana-derived continental blocks caused the disintegration of the Western Tethys Ocean (Rögl, 1998). It fragmented into the Mediterranean Sea (the southern domain) and Paratethys

(the northern domain) that were connected to each other and to the Atlantic and Indian Oceans through marine gateways (Rögl, 1998; Popov et al., 2004). As the starting point for the configuration of the basins in our model (Fig. 1), we use the Early Miocene paleogeography of Paratethys and the Mediterranean Sea, in which both are still connected to the Indian Ocean (e.g., Rögl, 1999). We treat Paratethys as a single basin, which is a reasonable assumption in view of the strong faunal similarities between the Eastern and Central Paratethyan domains (Rögl, 1998, 1999). The intricate paleogeography is simplified to a 4-box model with four gateways to achieve a simple quantitative setup capable of predicting the first-order response to gateway closure (see Fig. 1b). The boxes represent the Atlantic Ocean, the Mediterranean Sea, Paratethys and the Indian Ocean. The Mediterranean Sea is considered to have three gateways: in the west between the Mediterranean Sea and the Atlantic Ocean, GMA; in the east between the Mediterranean Sea and the Indian Ocean, GMI; and in the north between the Mediterranean Sea and Paratethys, GMP. Paratethys is considered to have two gateways: with the Mediterranean Sea, GMP; and a gateway to the Indian Ocean, GPI. Paratethys lacks a direct connection to the Atlantic Ocean. We aim to determine the evolution of salinity and temperature of both the Mediterranean Sea and Paratethys (S_M , T_M , S_P and T_P) before and after closure of the gateways to the Indian Ocean (i.e., closure of GMI and GPI). In Section 2.2, we provide a qualitative description of the basic concepts of our 4-box model.

2.2. Underlying concepts

Similar to previous oceanic box models (e.g., Stommel, 1961; Meijer, 2006; Karami et al., 2009) each box in our model is assumed to be well mixed and therefore it has a uniform salinity and temperature. The boxes associated with the Atlantic and Indian Oceans are taken to be two large reservoirs: their salinity and temperature are prescribed and kept constant during the simulations. It is assumed that the boxes exchange water through the gateways by means of a two-layer flow: a deep flow and a surface flow moving in opposite directions. The deep flow is parameterized as a function of the pressure difference between the two boxes which, by applying the common assumption of hydrostatic balance, is proportional to the density difference between boxes. Hence, the deep flow goes from the denser box (colder and/or more saline) into the less dense one (warmer and/or less saline). Mathematically, deep flow is given by the multiplication of the density difference and a parametric quantity known as the hydraulic constant. The hydraulic constant represents the geometry of the gateway. A larger hydraulic constant represents a deeper and/or wider gateway and vice versa. The surface flow is found from the requirement that water volume be conserved. Our formulation allows for surface and deep flow not being

equal in magnitude for a given gateway. This allows a net flow through the gateways depending on the ratio of the exchange flow in the eastern gateways to that in the western ones. Generally, at least a small net flow into or out of the Mediterranean and Paratethyan boxes is required to preserve their volume in the presence of a real freshwater exchange with the atmosphere.

We apply conservation of water mass and the equations of salt and heat balance to the Mediterranean Sea and Paratethys. Atmospheric forcing is imposed on Mediterranean and Paratethyan boxes as (i) net evaporation (i.e., the difference between evaporation E , precipitation P and river discharge R , i.e., $E-P-R$) and (ii) surface heat flux (Q). We use net evaporation as a real freshwater input instead of a virtual salinity flux (cf. Stommel, 1961). Net evaporation ($E-P-R$) is a term in the conservation of mass equations and surface heat flux (Q) is a source/sink term in heat balance equations. Salt and heat are advected through surface and deep flows into and out of the Mediterranean Sea and Paratethys as described by simple linear laws. The resulting system of equations for salinity and the temperature of Paratethys and the Mediterranean is solved, through time, in terms of various control parameters to find the steady state solution. From this we subsequently determine the configuration of exchange flows. The equations that represent these concepts are derived in the Appendix A.

2.3. Implementation of the exchange flows with the Indian Ocean

To investigate the role of closure of the gateways between the Mediterranean/Paratethys and the Indian Ocean (i.e., GMI and GPI) we allow only these gateways to vary while the other gateways (GMA and GMP) are kept constant during a single model run. We define the hydraulic constant for the variable gateways GMI and GPI (i.e., f_{MI} , f_{PI}) relative to the hydraulic constant of the invariable gateways (i.e., f_{MA} , f_{MP}). The ratios between these hydraulic constants are r_M (f_{MI}/f_{MA}) and r_P (f_{PI}/f_{MP}) for the Mediterranean Sea and Paratethys, respectively. As r_M and r_P approach zero, the deep flows to or from the Indian Ocean become zero. Moreover, we define the ratio of surface flow in GMI to the surface flow in GMA as r_M^s and ratio of surface flow in GPI to the surface flow in GMP as r_P^s (where superscript “s” refers to surface flow). Choosing r_M^s and r_P^s to be zero means that the surface flows to or from the Indian Ocean are zero. To simulate closure, we decrease all the gateway ratios (i.e., r_M , r_P , r_M^s and r_P^s) to zero. The model variables (the salinity and temperature of the Mediterranean and Paratethys) and model parameters are listed in Table 1 and Table 2, respectively.

No data or other independent constraints on the magnitude of exchange flows with the Indian Ocean exist. This results in four unknown control parameters (i.e., r_M , r_P , r_M^s and r_P^s) with an infinite number of possibilities to determine the exchange flows. To decrease the number of unknown parameters we concentrate our analysis on two cases: (i) equal surface and deep flow in the gateways to the Indian Ocean, and (ii) surface flow only in these two connections. These cases correspond to the ratio of surface to deep flow with the Indian Ocean being unity or infinity, respectively. Hence, we cover the limits of the range of possible solutions for the ratio of surface to deep flow with the Indian Ocean. In the first case, the surface flow ratios (i.e., r_M^s and r_P^s) can be written as a function of the corresponding deep flow ratios (i.e., r_M and r_P) and so they can be eliminated from the equations. Note that the surface flows between the Mediterranean and the Atlantic Ocean, and between the Mediterranean and Paratethys are not equal to the corresponding deep flows because volume has to be conserved. The main results presented below prove not to be very sensitive to the

Table 1
Definitions of the model variables.

Variables	Symbol
Salinity and temperature of the Mediterranean (psu, °C)	S_M, T_M
Salinity and temperature of the Paratethys (psu, °C)	S_P, T_P

Table 2
Definitions of the model parameters.

Variables and parameters	Symbol
Volume of the Mediterranean Sea (m^3)	V_M
Volume of the Paratethys (m^3)	V_P
Salinity and temperature of the Atlantic Ocean (psu, °C)	S_A, T_A
Salinity and temperature of the Indian Ocean (psu, °C)	S_I, T_I
Net evaporation over the Mediterranean Sea (m^3/s)	$(E-P-R)_M$
Net evaporation over the Paratethys (m^3/s)	$(E-P-R)_P$
Net surface heat flux over the Mediterranean Sea (W)	Q_M
Net surface heat flux over the Paratethys (W)	Q_P
Hydraulic constant for gateways connecting the Mediterranean to Atlantic and Indian Ocean (m^3/s)	f_{MA}, f_{MI}
Hydraulic constant for the gateway connection the Paratethys to the Mediterranean Sea or the Indian Ocean (m^3/s)	f_{MP}, f_{PI}
Ratio of the hydraulic constant of the eastern gateway of the Mediterranean to that of the western gateway (f_{MI}/f_{MA})	r_M
Ratio of the hydraulic constant of eastern gateway of the Paratethys to that of the western gateway (f_{PI}/f_{MP})	r_P
Ratio of the surface flow from the Indian Ocean into the Mediterranean to the surface flow in/out the Atlantic	r_M^s
Ratio of the surface flow from the Indian Ocean into the Paratethys to the surface flow in/out the Mediterranean	r_P^s
The ratio of surface to deep flow at the gateways to the Indian Ocean	h

choice of equal surface and deep flow to and from the Indian Ocean (see Discussion section). In the second case, with only surface flow, the deep branch of exchange with the Indian Ocean is taken as zero ($r_M = 0$ and $r_P = 0$) and as a result there is only one-layer flow to or from the Indian Ocean. This case relates to the advanced stage of Arabia-Eurasia collision, for which paleogeographic maps show long and shallow gateways between the Mediterranean Sea and the Indian Ocean, and between Paratethys and the Indian Ocean (Popov et al., 2004; Reuter et al., 2009). It is conceivable that such gateways accommodated one-way flow.

2.4. Model parameters

Here, we introduce the model parameters that are consistent in all model experiments. The remaining parameters that vary will be discussed in Section 3.

The volumes of Paratethys and the Mediterranean Sea prior to closure are approximated by taking the coastlines from the Early Miocene paleogeographic map of Meulenkamp and Sissingh (2003) and assuming an average depth of 1500 m (which is the average depth of the present-day Mediterranean) for each basin. We find $3 \times 10^{15} m^3$ and $6 \times 10^{15} m^3$ for Paratethys and the Mediterranean Sea, respectively. Although these are rough estimates at best and the volume of Paratethys and the Mediterranean changed during the Miocene, it can be shown that changes in volume do not affect our results. Mathematically, volume is the coefficient of the term for the first derivative of salinity and temperature to time (for the first order differential equation) which controls only the time to reach equilibrium and it does not influence the steady state solutions (see Eqs. (1)–(4) in Appendix A).

The boundary conditions for temperature and salinity of the inflow water, i.e., salinity and temperature of the Atlantic and Indian Oceans (S_A, S_I, T_A , and T_I), also need to be estimated since their exact values in the Miocene are not known. We set the Atlantic Ocean to $S_A = 36$ psu and $T_A = 16$ °C, which are approximately the present-day average values for the Atlantic inflow to the Mediterranean Sea (Hopkins, 1999). We assume that the Indian Ocean is warmer and less saline than the Atlantic Ocean (Stewart et al., 2004; von der Heydt and Dijkstra, 2006). According to von der Heydt and Dijkstra (2006), the sea surface salinity and temperature difference between the Indian and the Atlantic oceans (δS and δT) are roughly equal to -2 psu and 5 °C, respectively. We apply these differences to our well-mixed

oceanic boxes and assume that $S_I = 34$ psu and $T_I = 21$ °C. Consequences of choosing alternative values are discussed in Section 5.1.

The hydraulic constant for GMA is taken to be $f_{MA} = 3$ Sv (Karami et al., 2009). This value, six times larger than the value appropriate for the present-day Gibraltar Strait, is chosen to get the exchange flows in the order of $O(1)$ (i.e., exchange flows of around 10 Sv or smaller; see Karami et al., 2009) and to capture the situation that, according to paleogeographic maps (e.g., Rögl, 1999), gateways of the Early Miocene were relatively large. We take GMP to be smaller than GMA as suggested by the same paleogeographic maps. The hydraulic constant (f_{MP}) is conjectured to be $f_{MP} = 0.1$ Sv. This would make GMP analogous to the Hormuz Strait (the strait connecting the Persian Gulf to the Gulf of Oman) which has a minimum width of 54 km and a depth varying between 40 and 90 m. We also consider the effect of choosing other values of f_{MP} in Section 5.1.

3. Results I: Sensitivity analysis

In this first part of the results we systematically explore the model parameter space to determine how the temperature and salinity of Paratethys and the Mediterranean Sea respond to closure of the gateways to the Indian Ocean. As expected from the requirement of volume conservation, net evaporation affects both salinity and temperature, and we place more emphasis on exploring the role of this parameter. In addition, we investigate the importance of surface heat flux, comparing its effects to that exerted by the gateways. Moreover, we also present the case of one-way flow in the eastern gateways. In Section 4, we will combine our model with the available data from Paratethys.

3.1. Effect of closure dependent on net evaporation

3.1.1. Zero net evaporation ($E = P + R$)

We start our analysis with zero net evaporation (i.e., $E - P - R = 0$) and zero surface heat flux (i.e., $Q = 0$) in both basins. We calculate salinity as well as the temperature of the Mediterranean Sea (S_M, T_M) and Paratethys (S_P, T_P) as a function of two ratios r_M and r_P (Fig. 2). Constriction of the gateways connecting the Mediterranean Sea or Paratethys to the Indian Ocean means decreasing r_M or r_P , respectively (recall that surface and deep flow were considered equal in these gateways). Salinity of both basins increases and their temperature decreases by closure of the gateways to the Indian Ocean (Fig. 2a, compare the values at $r_M = 0$ and $r_P = 0$ to that for ratios greater than zero). The reason for this response is that the Indian Ocean acts as a source of warm and less saline water for the Mediterranean Sea and Paratethys, given that it is assumed warmer and less saline than the Atlantic Ocean. In addition, temperature and salinity of the two basins changes non-linearly in response to closure. That is, the smaller the gateways, the stronger the response to closure. Furthermore, by looking at each basin individually, we find that salinity and temperature of the Mediterranean Sea (S_M, T_M) are much more sensitive to closure of the gateway between the Mediterranean Sea and the Indian Ocean (i.e., decreasing r_M) than it is to closure of the gateway between Paratethys and the Indian Ocean (i.e., decreasing r_P). The Mediterranean Sea is connected to the Atlantic Ocean and the influence of Paratethys is relatively small. In contrast, salinity and temperature of Paratethys (S_P, T_P) are sensitive to the closure of both gateways (decreasing r_M and r_P) because the flow between Paratethys and the Mediterranean Sea is comparable in magnitude to the flow between Paratethys and the Indian Ocean. Any changes in the Mediterranean Sea will affect the exchange

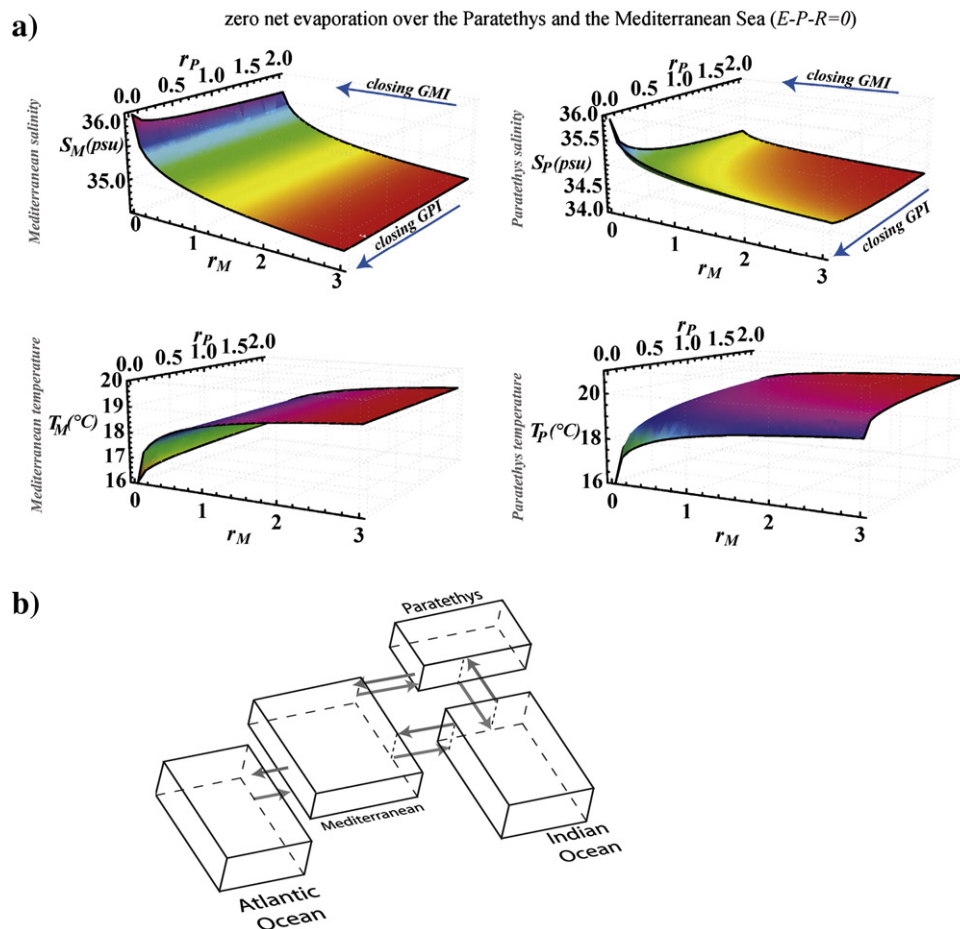


Fig. 2. a) Salinity and temperature of the Mediterranean Sea and Paratethys as a function of exchange flow with the Indian Ocean (r_M, r_P) for the case of zero net evaporation. b) Flow configuration for this experiment.

flow with Paratethys and thus influence Paratethys. Closing the Mediterranean Sea-Indian Ocean gateway can therefore alter the temperature and salinity of Paratethys.

In terms of the configuration of exchange flows (Fig. 2b) we find that the deep flow is from the Atlantic Ocean to the Mediterranean Sea and from there to Paratethys and the Indian Ocean. The surface flows

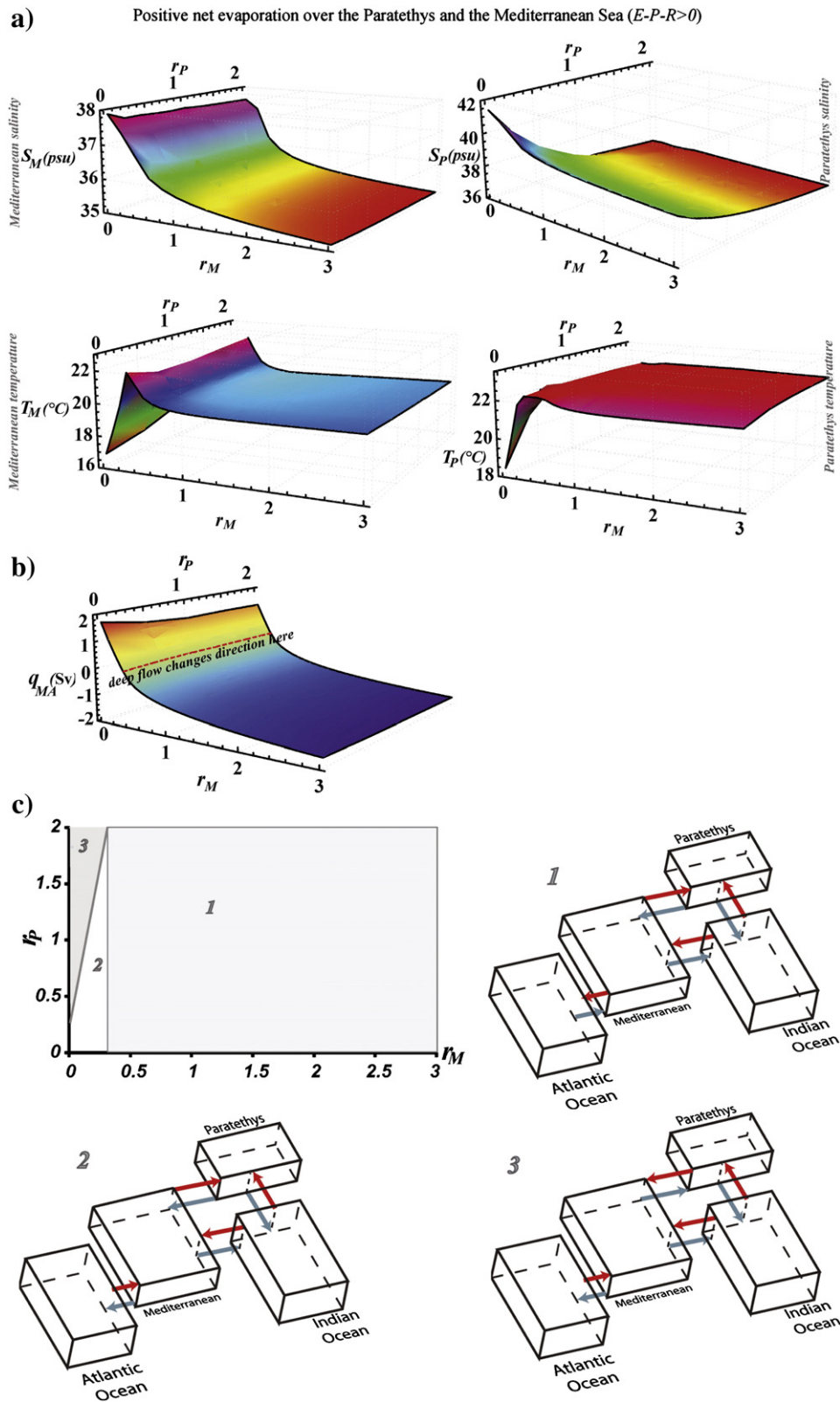


Fig. 3. a) Salinity and temperature of the Mediterranean Sea and Paratethys as a function of exchange flow with the Indian Ocean (r_M, r_P) for the case of positive net evaporation ($E-P-R = 1$ m/yr). b) Deep flow between the Mediterranean Sea and the Atlantic Ocean is shown by q_{MA} . Negative values correspond to the deep flow from the Atlantic Ocean to the Mediterranean Sea and vice versa; red dashed line shows the boundary where q_{MA} changes direction. c) Flow configuration is plotted as a function of two ratios r_M and r_P . Each region corresponds to a different flow configuration, labeled 1 to 3 and illustrated next to the graph. (For interpretation of the references to color in this figure legend, the reader is referred to the web version of this article.)

are from the Indian Ocean to Paratethys and the Mediterranean, and from the Mediterranean Sea toward the Atlantic Ocean.

3.1.2. Positive net evaporation ($E > P + R$)

Next, we consider the case in which evaporation exceeds precipitation and river discharge. We chose $E - P - R = 1$ m/yr for both basins which is in the range of estimated net evaporation for the present-day Mediterranean Sea (Hopkins, 1999). Compared to the case of zero net evaporation, there is an overall increase in both salinity and temperature of Paratethys (Fig. 3a). Positive net evaporation appears as a source term for both salinity and temperature and increases the flow of salt and heat into Paratethys (see Appendix A). For the same reason, this behavior is also found for the salinity and temperature of the Mediterranean but here changes are smaller. Upon closure, salinity of both the Mediterranean Sea and Paratethys increases and their temperature decreases, similar to the previous case. Salinity in this case shows a larger increase due to the positive net evaporation. Temperature shows more non-linear behavior than salinity: it is relatively constant for $r_M > 1$, then it increases for $r_M < 1$, and finally it falls sharply for $r_M < 0.3$. The non-linearity is more pronounced in the Mediterranean Sea than in Paratethys. This behavior is the result of the competition between the warmer water of the Indian Ocean and the colder water of the Atlantic Ocean. Provided there is a sufficiently large connection to the Indian Ocean ($r_M > 1$), the Mediterranean is at first less dense than the Atlantic Ocean because it is significantly warmer. Mediterranean salinity and therefore its density increases by constricting the gateways to the Indian Ocean (i.e., decreasing r_M and r_P) which in turn decreases the deep flow from the Atlantic Ocean, because density difference between the Mediterranean and the Atlantic Ocean is decreased (Fig. 3b). Consequently, for $0.3 < r_M < 1$, the warm Indian-Ocean inflow becomes dominant and raises

the temperature of the Mediterranean Sea. In turn, this increase in the Mediterranean temperature raises slightly the temperature of Paratethys. Further constriction of the eastern gateways ($r_M < 0.3$) decreases the Indian-Ocean inflow even more but the exchange flow with the Atlantic Ocean starts to increase since from this point onwards the Mediterranean Sea becomes more dense than the Atlantic Ocean because of its higher salinity. More inflow of cold Atlantic water makes both the Mediterranean Sea and Paratethys colder. This significant finding for the positive net evaporation scenario means that temperature remains relatively constant in the early stage of restriction but a warming trend ($\sim +1$ °C) followed by a sudden cooling (~ -5 °C) are to be expected as complete closure approaches in the advanced stage. As for the previous case, salinity and temperature of the Mediterranean Sea (S_M, T_M) are only sensitive to the changes of GMI. Paratethys temperature (T_P) is responsive to the closure of both gateways, GMI and GPI, but its salinity (S_P) is more sensitive to the closure of GPI than to closure of GMI.

The configuration of the exchange flow for this case is more complex than in the previous case and depends on the value of the ratios r_P and r_M (Fig. 3c). For example, deep flows (blue arrows) are from Paratethys to the Mediterranean Sea and the Indian Ocean—and from the Mediterranean Sea to the Indian and Atlantic Ocean for $r_P < 0.3$ and $r_M < 0.3$ (area 2 in Fig. 3c). Around $r_M \approx 0.3$, the exchange flow with the Atlantic Ocean reverses (going from area 2 to area 1) and this is the point where a sudden decrease in temperature occurs.

3.1.3. Negative net evaporation ($E < P + R$)

In the case where evaporation is less than the sum of precipitation and river discharge ($E - P - R = -1$ m/yr) there is an overall decrease in both salinity and temperature of Paratethys and the Mediterranean water compared to the previous cases (Fig. 4). The negative net evaporation acts

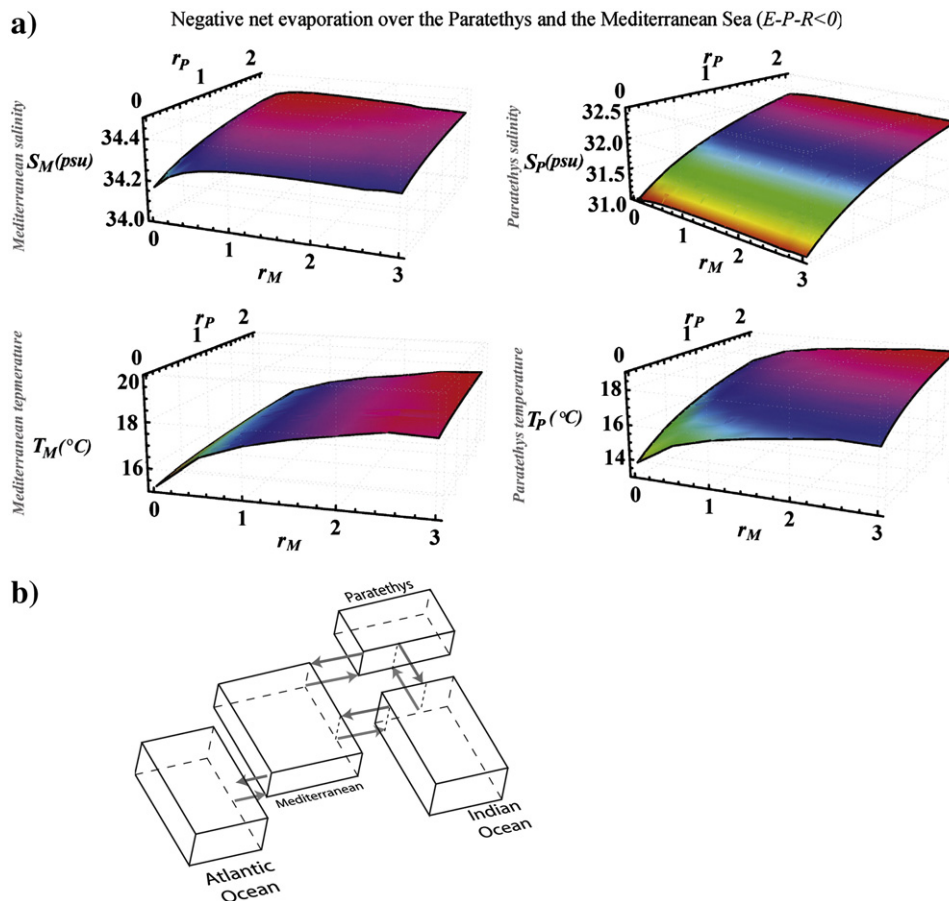


Fig. 4. a) Salinity and temperature of the Mediterranean and Paratethys as a function of exchange flow with the Indian Ocean (r_M, r_P) for the case of negative net evaporation ($E - P - R = -1$ m/yr). b) Flow configuration for this setup.

as a sink term for both salinity and temperature and decreases the flow of salt and heat into Paratethys and Mediterranean. Both the salinity and temperature of the Mediterranean Sea and Paratethys decrease during constriction of the Indian Ocean gateways. Salinity of the Mediterranean Sea displays a minor decrease in comparison with temperature which decreases significantly. The reason that salinity decreases in contrast to the cases with zero or positive net evaporation is the input of atmospheric fresh water. As before, the Mediterranean properties are mainly sensitive to restriction of the gateway between the Mediterranean Sea and the Indian Ocean. In contrast to the previous cases, the salinity of Paratethys does not respond to the closure of the gateway between the Mediterranean Sea and the Indian Ocean (GMI) and is only a function of the gateway between Paratethys and the Indian Ocean (GPI) (Fig. 4). The reason is that by constricting GMI (decreasing r_M) input of salt from the Mediterranean to Paratethys remains nearly constant. By contrast, the temperature of Paratethys is sensitive to constriction of both gateways.

The configuration of exchange flow in this case (Fig. 4b) is not as complex the case of positive net evaporation and does not change while constricting the gateways to the Indian Ocean. The deep flow is from the Atlantic Ocean to the Mediterranean Sea and from there to Paratethys and to the Indian Ocean; surface flow is in the opposite direction. In addition, there is a deep flow from the Indian Ocean to Paratethys, again with opposed surface flow.

3.1.4. Net evaporation pattern similar to that at present

Here we study the case where there is positive net evaporation over the Mediterranean Sea ($E-P-R = 1$ m/yr) and negative net evaporation over Paratethys ($E-P-R = -1$ m/yr). This case can be thought of as an approximate analog to the present-day Mediterranean and Black Sea system but with open gateways to the Indian Ocean. By constricting of

the gateway between the Mediterranean Sea and the Indian Ocean, GMI (decreasing r_M), salinity increases and temperature decreases in both basins (Fig. 5a). The increase in the salinity of Paratethys, in contrast to the previous case with negative net evaporation over the whole region, is related to the positive net evaporation over the Mediterranean which makes the inflowing water from the Mediterranean to Paratethys more saline. Constricting the gateway between Paratethys and the Indian Ocean, GPI (decreasing r_P), does not affect the Mediterranean Sea but does reduce the salinity and temperature of Paratethys. Of particular interest is the fact that the salinity of Paratethys is less sensitive to closure of GPI for restricted GMI (plane of constant r_M in Fig. 5a with $r_M \ll 1$). For example at $r_M = 3$, the salinity of Paratethys decreases by approximately 1 psu over a r_P range from 2 to 0, but at $r_M = 0$, salinity decreases by 0.2 psu over the same r_P range. The reason for this is that constricting GMI makes the salinity of Paratethys of the same order as the salinity of the Indian Ocean. This decreases the impact of exchange with the Indian Ocean on the salinity of Paratethys. Mathematically speaking, the source and sink terms related to the exchange with the Indian Ocean cancel each other in the equation concerning the salinity of Paratethys. Note that is not the case for the temperature of Paratethys. We conclude that closure of GPI alone does not affect the salinity of Paratethys because of the reduced sensitivity to the GPI in comparison with the previous cases.

Concerning the exchange flow in this case, there are two different configurations for $r_M > 0.2$ and $r_M \leq 0.2$ (Fig. 5b). In the first case ($r_M > 0.2$), deep flow is from the Atlantic Ocean to the Mediterranean Sea and to the Indian Ocean with opposed surface flow. However, in the second case, deep flows are directed from the Mediterranean to the Atlantic and to the Indian Ocean. In both cases, deep flows are into Paratethys with opposed surface flows. At $r_M \approx 0.2$, the exchange flow

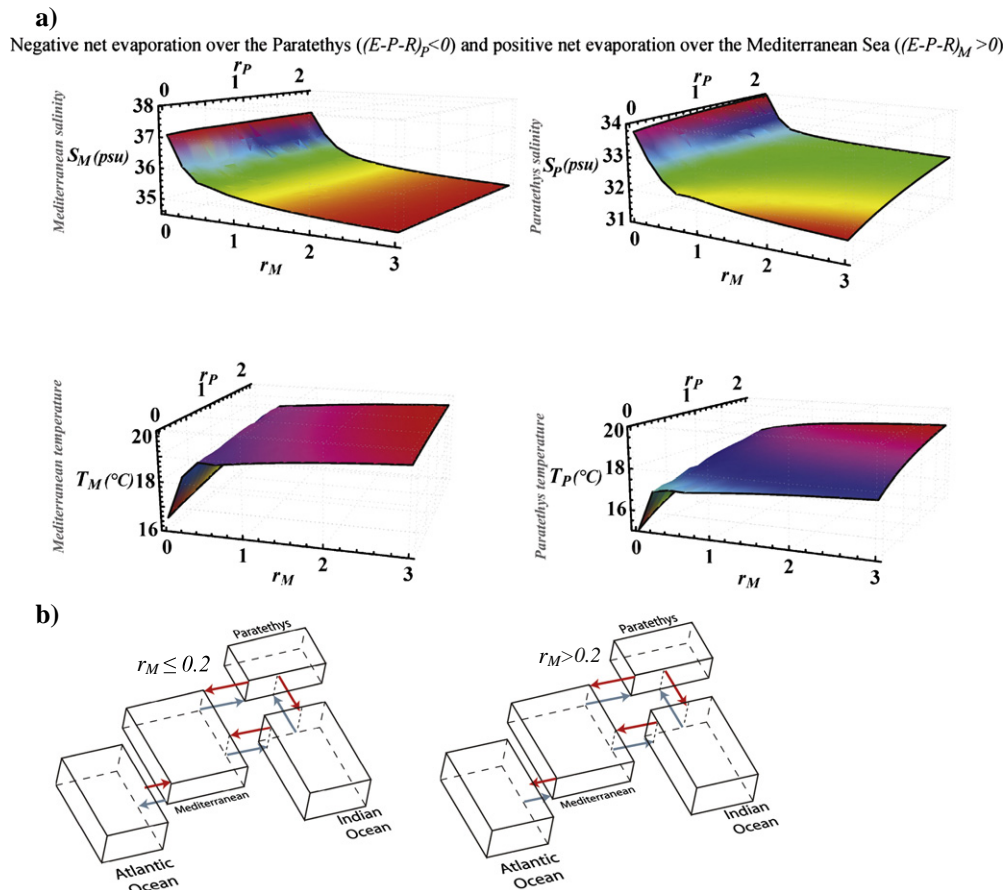


Fig. 5. a) Salinity and temperature of the Mediterranean and Paratethys as a function of exchange flow with the Indian Ocean (r_M, r_P) for the case of positive net evaporation ($E-P-R = 1$ m/yr) over the Mediterranean Sea and negative net evaporation ($E-P-R = -1$ m/yr) over Paratethys. b) Flow configuration for this setup.

between the Mediterranean and the Atlantic Ocean reverses and this is the point where a sharp slope in salinity and temperature occurs (Fig. 5b).

3.2. The surface heat flux (Q) versus gateways

In the results shown so far, the total surface heat flux (Q) was prescribed as zero. Here, we examine the role of surface heat flux and its importance relative to that of the gateways. We solve temperature and salinity as a function of surface heat flux Q and gateway ratios r_P and r_M . The latter ratios are taken to be equal (i.e., $r_P = r_M$). This is convenient because it reduces the number of parameters and can be shown that does not have an important effect on the results described in this section. We consider a range for Q of both basins between -5 W m^{-2} and 5 W m^{-2} . To put this in perspective, the present-day yearly-averaged net surface heat flux of the Black Sea and the Mediterranean Sea are 0.0 W m^{-2} and -5 W m^{-2} , respectively (Hopkins, 1999; Kara et al., 2008). In our model, a positive surface heat flux for a given basin means warming up the basin and vice versa. For the model parameters we use the same values as before. We prescribe a value for net evaporation over both basins.

Fig. 6 shows temperature of the Mediterranean and Paratethys as a function of surface heat flux (Q) and corresponding gateway ratio (r_P or r_M) for different values of net evaporation. Salinity proves quite insensitive to changes in surface heat flux and is not shown. In our model, because the net evaporation and surface heat flux are acting independently, surface heat flux can only affect salinity indirectly through its influence on the exchange flow. This effect proves to be small for Paratethys and negligible for the Mediterranean. In contrast, the temperature of the basins is directly influenced by the heat flux since this flux is introduced as a source/sink term in the equations for temperature. The response of temperature to variation in Q depends on the size of the gateway connecting to the Indian Ocean i.e., size of r_P or r_M (plane of constant r_P or r_M in Fig. 6). The larger the gateways (larger r_P or

r_M), the less sensitive the basins become to variation of the surface heat flux. A larger exchange flow with the open ocean suppresses the effect of atmospheric heat flux. Temperature of the Mediterranean Sea (T_M) is relatively insensitive to the variation of Q before closure (plane of constant r_M with $r_M \gg 0$ in Fig. 6) but it becomes highly responsive for limited exchange and complete closure ($r_M \approx 0$). The temperature of Paratethys (T_P), on the other hand, varies significantly by changing Q even before closure (plane of constant r_P with $r_P \gg 0$ in Fig. 6) although it also displays greater sensitivity close to complete closure ($r_P \approx 0$). Paratethys is more sensitive to the variation of Q than the Mediterranean Sea due to its more restricted connections with the open ocean. By decreasing the connection to the Indian Ocean (decreasing r_P or r_M) while keeping Q constant (the plane of constant Q in Fig. 6), temperature of the Mediterranean Sea, except for the cases with $E-P-R = 1 \text{ m/yr}$ and $Q > 3 \text{ W/m}^2$, decreases for most values of Q . Moreover, the temperature of Paratethys decreases for all values of $Q < 3 \text{ W/m}^2$. However, if Q increases, e.g., from a negative value to a positive one while constricting the gateways, the Mediterranean Sea and especially Paratethys become warmer.

3.3. One-way flow in the eastern gateways

In our model formulation we represent this case by $r_P = 0$ and $r_M = 0$. In contrast with the previous cases, the equations are solved as a function of the surface flow ratios i.e., r_M^s and r_P^s . The solutions are only shown for the range $r_P^s \leq 1$ and $r_M^s \leq 1$, which is most likely given that we are dealing with shallow gateways. It should be also noted that some flow configurations do not have valid solutions for $r_P^s > 1$ and $r_M^s > 1$ due to the requirement of conservation of mass. We present two cases for net evaporation over the basins: (i) negative net evaporation over both basins and (ii) positive net evaporation over Paratethys and negative over the Mediterranean Sea. Other combinations of net

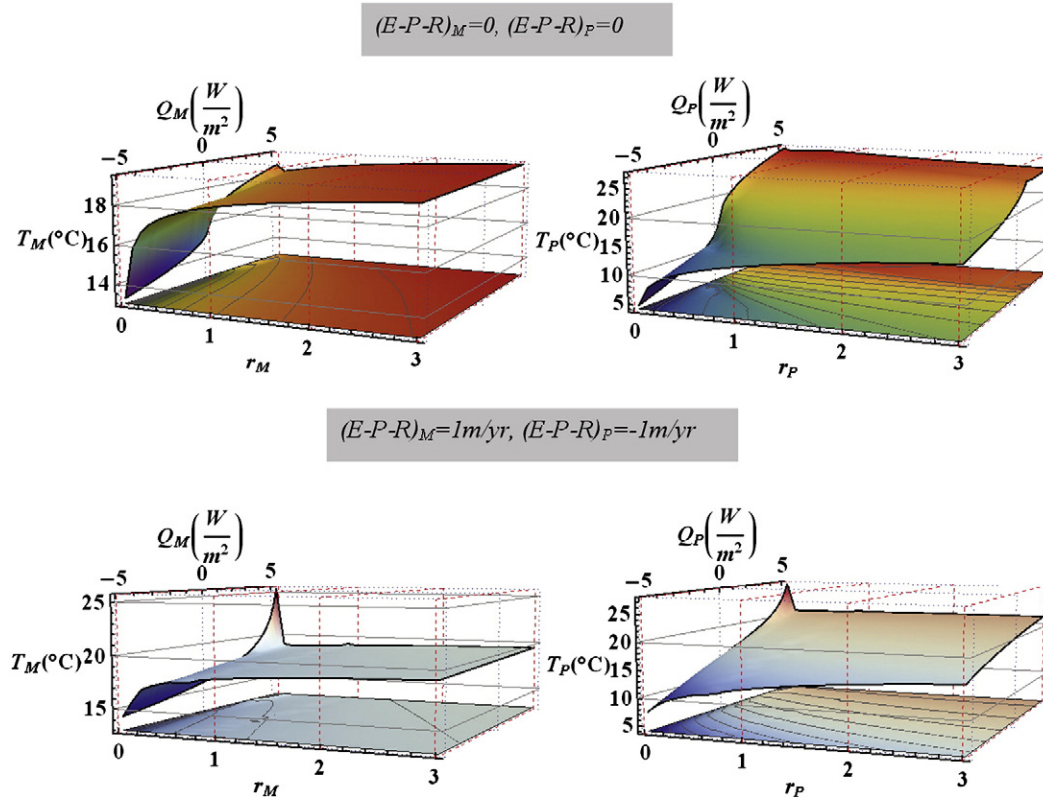


Fig. 6. Temperature of the Mediterranean Sea (T_M) and Paratethys (T_P) as a function of their net surface heat flux (Q_M and Q_P) and gateway ratios (r_M or r_P). Upper panel: for zero net evaporation; lower panel: similar to present-day system. To clarify the figure we also show the 3-D surface projected on the bottom face of each graph using contour lines. Note, a positive Q means warming of the basin, a negative Q implies basin cooling.

evaporation yield results similar to the corresponding two-layer flow cases and are not shown.

In the case of positive net evaporation over Paratethys and negative over the Mediterranean Sea, Mediterranean properties and the salinity of Paratethys are dependent on r_M^s but insensitive to r_P^s (Fig. 7). The temperature of Paratethys, however, is sensitive to variation of both r_M^s and r_P^s . The reason that the temperature of Paratethys is sensitive to r_P^s but not salinity is the result of a) the configuration of the exchange flow and b) the difference between the Indian and the Mediterranean (the basins connected to Paratethys) in terms of salinity and temperature. Surface flows are from both Mediterranean and Indian Ocean into Paratethys. The surface flow from the Mediterranean, which is colder and more saline, increases by decreasing the surface flow from the Indian Ocean (i.e., decreasing r_P^s) because the volume of Paratethys must be conserved. The difference between the Mediterranean and Indian in terms of salinity (~1 psu) is smaller than their difference in temperature (~5 °C) and this causes the temperature of Paratethys to be more affected.

In the case of negative net evaporation over both basins, both Mediterranean and Paratethys water properties are dependent on the surface flow between the Mediterranean and the Indian Ocean (i.e., dependent on r_M^s). On the other hand, these properties are independent of the surface flow between Paratethys and the Indian Ocean (i.e., independent of r_P^s). The reason for this behavior is related to the surface flows from Paratethys to both Indian Ocean and Mediterranean Sea. The decrease in the surface flow to the Indian Ocean (decrease in r_P^s) is compensated by increased surface flow to the Mediterranean to conserve mass, and therefore water properties of Paratethys are not affected. The important implication is that, for the case of negative net evaporation, opening or closure of a shallow gateway between Paratethys and the Indian Ocean will not affect Paratethys salinity and temperature.

3.4. Summary of the results

To summarize, we studied salinity and temperature of the Paratethyan and Mediterranean Seas prior to closure and the changes

due to closure for various values of model parameters. We found that water properties of Paratethys are sensitive to both Paratethys–Indian and Mediterranean–Indian gateways but those of the Mediterranean are sensitive mainly to the Mediterranean–Indian gateway. While net evaporation is kept constant, the temperature of both Paratethys and the Mediterranean Sea decreases upon closure. This is found for various values of net evaporation. Decrease in net evaporation (i.e., from positive to negative values) while constricting gateways, can enhance the cooling effect of closure and vice versa. Salinity, however, decreases or increases upon closure depending on the value of net evaporation. The cooling effect induced by closure is found for most values of surface heat flux (e.g., $Q < 3 \text{ W/m}^2$) where the heat flux is kept constant during closure. However, by increasing Q and constricting the gateways simultaneously, the cooling effect of closure is suppressed. Cooling is enhanced when Q is decreased. Moreover, we studied the case of one-way flow in the eastern gateways. Opening (closing) a gateway with one-way flow induces a greater warming (cooling) than two-way flow case.

Generally, semi-enclosed seas with a limited connection to the open ocean exhibit increased sensitivity to climate change and vice versa. When the basins exchange less water with the open ocean, the atmospheric forcing (net evaporation and heat flux) becomes more dominant. The opposite is true when basins exchange large amounts of water with the open ocean. Furthermore, in a basin with more than one gateway, changes in one gateway can alter the water properties of the basin significantly if the two gateways accommodate approximately the same amount of exchange flow. If the gateway subject to change is much smaller (e.g., ten times shallower) than the other, its variation will have little impact on the water properties.

4. Results II: The impact of gateway changes on the temperature of the Central Paratethys

Our results demonstrate that closure of the gateways connecting Paratethys and the Mediterranean to the Indian Ocean has a great impact on the basins' temperature as well as on their salinity. Here we compare the model-predicted changes in temperature with those

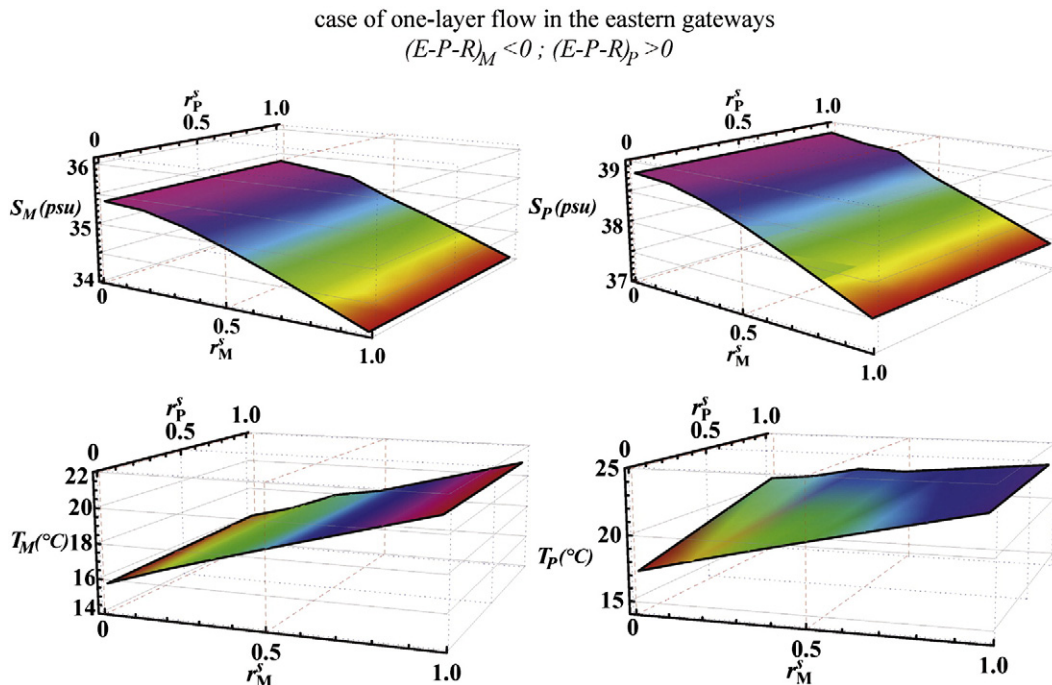


Fig. 7. Salinity and temperature of the Mediterranean Sea and Paratethys as a function of the surface flow ratios (r_M^s and r_P^s). This case corresponds to the case of one-layer flow in the gateways connecting to the Indian Ocean. Net evaporation is positive for Paratethys and negative for the Mediterranean Sea.

inferred from the geological record to understand the role of gateways in causing such changes. The focus is on the Central Paratethys because a wealth of Early to Middle Miocene geological data is readily at hand for this region which makes it an ideal test case. Model-predicted salinity is not evaluated because no paleo-salinity data are currently available. We first summarize the temperature proxy record of the Central Paratethys to reconstruct its temperature evolution. Subsequently, the state of gateways (open or closed gateways) to the Indian Ocean during the Miocene is addressed and used in our model to assess the associated impact on water temperature. The model results are then compared against the observed temperature.

4.1. Proxy data for the Miocene temperature evolution of the Central Paratethys Sea

Temperature estimates for the Central Paratethys mostly rely on a comparison of the biota characteristic for a certain time interval with their present-day relatives. We compile data from the Burdigalian to Serravallian of the Central Paratethys and leave out the earlier stage of the Aquitanian because of the low number of available data. In addition to the common global stages, we will also make reference to the regional stages for the Central Paratethys, such as Eggenburgian, Ottnangian, Karpatian and Badenian (Fig. 8). A number of isotope and trace element studies are also available for the time period considered. However, a direct interpretation of these records in terms of paleo-temperature without a consistent control based on the faunal record is risky (Latal et al., 2006). The reason is that small marginal seas such as Paratethys can be strongly influenced by regional differences in seawater isotope compositions (Latal et al., 2006; Harzhauser et al., 2007b). We have thus chosen to rely almost exclusively on faunal assemblage records for seawater temperature reconstruction. The proxy data used for temperature reconstruction relate to different parts of the prior sea and may refer to different depth levels. We will nevertheless combine the available observations to obtain an estimate (minimum and maximum values) of the temperature representative of the whole basin for a specific stage. This approach matches the fact that our model solves for a single basin-averaged temperature. It is supported by the inference, based on oxygen isotopes of benthic and planktonic foraminifera, that Paratethys was well mixed prior to the late Badenian (Baldi, 2006). In any case, we will work with the full range of inferred temperatures and be emphasizing trends in change, rather than absolute values. Often, proxy-derived temperature estimates are given only in qualitative terms (e.g., “tropical” or “temperate”) and suggested temperature ranges for these terms are not consistent in various studies. We combined a series of papers and attribute a numeric temperature range to each of these qualitative terms as follows: “cool-temperate” is 10–15 °C, “temperate” (mild-temperate) is 15–17 °C, “warm-temperate” is 17–21 °C, “sub-tropical” is 21–25 °C, and tropical is 25 °C and larger (Hall, 1964; Burns and Nelson, 1981; Kamp et al., 1990; Pocknall, 1990; Ogasawara, 1994).

In the early Burdigalian (middle and late Eggenburgian), a highly diverse echinoid fauna (Kroh, 2007) and tropical mollusc assemblages (Mandic and Steininger, 2003; Mandic et al., 2004) are indicative of warm-temperate to tropical water (17–25 °C). Harzhauser et al. (2007b) suggested a minimum temperature of around 15 °C for this period based on molluscs and sedimentological and isotope data. This gives rise to a first time–temperature estimate (P1) in the graph shown in Fig. 8a (the upper limit is uncertain; the horizontal bar is centered arbitrarily).

Bryozoan–coralline limestones, previously assigned to the late Eggenburgian (Nebelsick, 1989) but recently attributed to the earliest Ottnangian (Piller et al., 2007). These are interpreted to indicate warm-temperate conditions (17–21 °C) and support a transition from warmer to colder conditions from the Early to the Middle Burdigalian. Bachmann (1973) suggested a maximum sea surface temperature (SST) of 15 °C for the middle Burdigalian (early Ottnangian) based on silicoflagellate

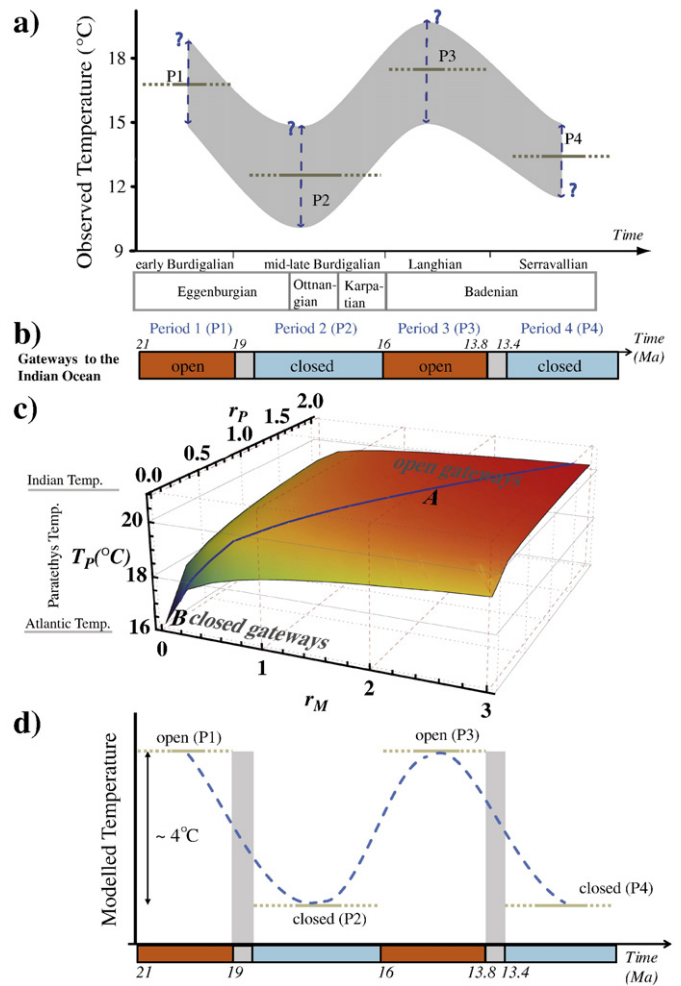


Fig. 8. Combination of data and model results for the evolution of Paratethyan temperature during the Miocene. a) The evolution of Paratethyan temperature is divided into four distinct periods shown as P1 to P4. The gray-shaded band, together with the horizontal and vertical dashed line segments, indicates the associated uncertainties. Paratethys regional stages are given below the standard (Mediterranean) Miocene stages. b) The state of gateways to the Indian Ocean during the Miocene. c) The temperature of Paratethys calculated as a function of gateway ratios r_M and r_P . This repeats the model result shown in Fig. 2a. Letters “A” and “B” identify solutions representing open and closed gateways, respectively. d) Variation in Paratethyan temperature between stages of open and closed gateways as found by modeling. The gray-shaded segments in panel b and panel c indicate the periods in which the paleogeography was very complex and the model is not applicable (see the text).

assemblages and the frequent occurrence of diatomites. Low planktonic $\delta^{13}\text{C}$ and rather high $\delta^{18}\text{O}$ values were found, suggesting high productivity and cold SST (10–14 °C; Grunert et al., 2010) but these may underestimate the real SST because they relate to paleoenvironmental setting of upwelling.

Cool-temperate water (10–15 °C) with high amounts of siliceous fossils (Rögl et al., 2003) was characteristic for the late Burdigalian (early Karpatian). Water conditions were found to be similar to those in the middle Burdigalian (Ottnangian; Harzhauser and Piller, 2007). Moreover, Cicha et al. (2003) suggested temperate water (14–17 °C) based on planktonic foraminifers. We conclude that the Central Paratethyan water was generally cold to temperate (~10–15 °C) in the middle and late Burdigalian (P2 in Fig. 8a).

In the latest Burdigalian, the temperature of Central Paratethys started to increase since warmer water foraminifers, such as Globigerinoides or Globorotalia and a thermophilic mollusc fauna (Harzhauser et al., 2003) appeared (late Karpatian). A minimum SST of 14 to 16 °C was estimated by Harzhauser (2002) for this period –

warmer than middle to late Burdigalian – based on a comparison of gastropods of the Korneuburg Basin with their modern stenothermic relatives. Temperature requirements of the corresponding fish (Reichenbacher, 1998; Schultz, 1998, 2003) and echinoid (Kroh, 2007) faunas also support warm-temperate and sub-tropical temperatures (17–25 °C).

For the Langhian (early Badenian) a minimum SST of 15–17 °C was estimated based on mollusc faunas (Harzhauser et al., 2003) and planktonic foraminifera (Gonera et al., 2000). The occurrence of several strombolid genera (Harzhauser et al., 2003) even suggests slightly higher SST of 16–18 °C (Latal et al., 2006). Early Langhian (early Badenian) gastropod (Harzhauser, 2002, 2003), bivalve (Mandic, 2003), pteropod (Bohn-Havas and Zorn, 2003), and echinoderm faunas (Kroh, 2003) were found similar to those of the latest Burdigalian (late Karpatian), but with strikingly higher diversity. The increase in faunal diversity is often explained to reflect a large immigration wave from the Mediterranean area in response to a rise in the temperature of Paratethys (Harzhauser et al., 2003; Mandic, 2003). There is a peak in diversity among foraminifers (Cicha et al., 1998; Ćorić et al., 2004) as well as echinoids. The latter are tropical in appearance and indicate a winter SST of 17 to 18 °C (Kroh, 2007). The climax in carbonate production and algal limestone deposition (Studencka et al., 1998; Filipescu, 2001), diversity of reefs in the southern parts of Paratethys and presence of several small coral reefs composed of *Montastrea*, *Tarbellastraea*, *Leptoseris* and *Porites* in the Styrian Basin (Harzhauser and Piller, 2007) all indicate warm climate in this period. Both fauna and depositional environment reflect a stable subtropical marine environment (Kováč et al., 2007). Thus, the Paratethyan water was generally warm-temperate to tropical during the Langhian (P3 in Fig. 8a). The time-temperature estimate for this period ranges between 15 °C and tropical (>25 °C).

Marine microfaunal assemblages indicate a climatic change from warmer water in the Langhian (early Badenian) to colder water in the Serravallian (middle and late Badenian; see P4 in Fig. 8a) (Dumitrică et al., 1975; Bicchi et al., 2003; Spezzaferri et al., 2004). Also changes in the echinoid fauna (Kroh, 2007) and a distinct change in reef structures (Harzhauser and Piller, 2007; Piller et al., 2007) indicate the drop in temperature. More moderate-water ostracodes appeared (Jiříček, 1983) and there was a slight increase in moderate-water gadoids (Brzobohatý et al., 2007). Toth et al. (2010) document stable bottom-water temperature (~15 °C) based on palaeontological and geochemical analyses of foraminifera, ostracods, gastropods and rodents. However, Harzhauser et al. (2007b) suggested even lower temperature for this period (~12 °C). The drop in temperature occurred just before evaporite deposition started throughout major parts of the Central Paratethys at 13.8 Ma (i.e., the earliest Serravallian following Hilgen et al., 2009; de Leeuw et al., 2010). Foraminiferal assemblages indicate that the fall in warm water taxa was much more pronounced in the Central Paratethys than in the Mediterranean (Bicchi et al., 2003). The time-temperature estimate for period P4 is thus 15 °C and lower.

In summary, the record of the Paratethyan temperature suggests that the evolution of the basin can be divided into four distinct periods (periods 1 through 4, defined as P1 to P4 in Fig. 8a). The temperature of Central Paratethys was warm-temperate to tropical during the early Burdigalian, cold to temperate from the middle to the late Burdigalian, becoming warm again (near tropical temperature) during the Langhian, and cold in the early Serravallian.

4.2. Model parameters applied

As stated before, the atmospheric forcing (i.e., net evaporation and heat flux) over Paratethys during the Early-Middle Miocene is not known. We apply the conditions used in Section 3.1.1, i.e., zero net evaporation and zero heat flux. In terms of net evaporation, this choice does not affect the qualitative behavior of temperature (see

Section 3) since different assumptions regarding net evaporation yield similar changes in temperature in response to closure. This means that although absolute values of Paratethys temperature vary, the difference between maximum temperature and minimum temperature is essentially the same. In terms of net surface heat flux, this choice is reasonable as we aim to focus on the effect of gateways.

4.3. The effect of gateway configuration on Central Paratethys temperature: model predictions

The model experiments require a specification of the gateways' states. They are derived from paleogeographic reconstructions and are based on the presence or absence of Indian Ocean elements in the fauna of the Mediterranean and Paratethys. Observations of the temperature of Paratethys compiled in Section 4.1 have not already, by the authors who reported these data, been tied to either an open or closed nature of the gateway to the Indian Ocean. The inferred gateway states (open or closed) for each of the periods that characterize the Paratethyan temperature (P1 to P4) are subsequently used in our model. The resulting model predictions for temperature are compared with the temperature evolution in Fig. 8a to assess the role of gateways in controlling the Paratethyan temperature. The short late middle Burdigalian (late Otnangian) and early Serravallian (middle Badenian) restriction events, gray area in the Fig. 8b, are beyond the scope of this paper and will not be considered. As stated before, our analysis is done mostly in regards to trends rather than absolute values.

During the early Burdigalian (P1 in Fig. 8b) the gateways to the Indian Ocean were open (Harzhauser et al., 2007a). Paleogeographic reconstructions depict the Paratethys as one large sea (Rögl, 1999) justifying the representation of the Paratethys as one box. We do not know the exact values of the gateway ratios r_M and r_P . However, the model indicates that, except for values smaller than about 0.3, the temperature is nearly independent of the ratios and amounts to about 20 °C (the plateau labeled "A" in Fig. 8c). It seems likely that the ratios were larger than 0.3 because the gateways to the Indian Ocean are shown as fairly large on the paleogeographic maps (e.g., Rögl, 1999; Meulenkamp and Sissingh, 2003). We thus find that the temperature of Paratethys is higher than that of the Atlantic in period P1. This matches well the geological evidence: the discussed proxy data for the early Burdigalian (i.e., Eggenburgian) indeed indicate relatively warm waters in the Paratethys (Fig. 8a).

In the middle to late Burdigalian (P2), the first closure of the gateways to the Indian Ocean occurred (Rögl, 1999; Harzhauser et al., 2007a; Reuter et al., 2009). The Eastern Paratethys became disconnected from the Central Paratethys (Rögl, 1999) and for much of P2, our model only applies to the Central Paratethys occupying a position equivalent to our fourth box. Our model results suggest that closure of the gateway to the Indian Ocean – i.e., going from A to B in Fig. 8c – resulted in cooling by about 3–4 °C (also schematically indicated in Fig. 8d). This cooling is again consistent with proxy-data. Importantly, no major coeval cooling is expressed in the global climatic record (Harzhauser et al., 2007b; Zachos et al., 2008). Thus, based on our box model analysis, we suggest that the hitherto enigmatic cooling event in Paratethys might be a regional effect resulting predominantly from the closure of the gateways between the Mediterranean/Paratethys and the Indian Ocean. It follows from the above that the transition from P1 to P2 not only involves closure of the Indian Ocean gateways but also, effectively, a reduction in volume of the Paratethys box. It can be shown that changes in volume do not play a role in the results of our model.

Just before the onset of the Langhian (P3; 16–13.8 Ma), the gateways reopened as indicated by the presence of marine sediments in the Mesopotamian Trough and the occurrence of foraminifera of Indo-Pacific affinity in the Paratethys (Rögl, 1999; Harzhauser et al., 2007a). With the advent of the Langhian, the Eastern and Central

Paratethys reconnect and the Paratethys can again be considered a single basin in period P3. We find that reopening of gateways to the Indian Ocean in P3 (i.e., going from B to A in Fig. 8c) should have resulted in warming of the Paratethys by about 3–4 °C. Proxy data indeed point at warming, but the magnitude of the increase (~6–8 °C) is greater than predicted. P3 does, however, coincide with the onset of the globally recognized Middle Miocene Climatic Optimum (MMCO; Harzhauser and Piller, 2007), associated with warming of the Atlantic and Indian Oceans. The Indian Ocean water entering the Paratethys and Mediterranean thus had a higher temperature than before. We therefore argue that the strong increase in Paratethys temperature registered consists of both a gateway-related component and a component induced by global climate change. Based on our model results, we reason that the registered increase in temperature should thus be stronger than would be expected based on global warming only.

An alternative explanation for the excessive increase in temperature apparent from proxy data relates to the mode of gateway flow. So far we considered that, after reopening, gateways accommodated a two-way flow. Note that reopening of the gateways with one-way flow (i.e., shallow gateways) causes higher temperature (~5–6 °C) in Paratethys than the two-way flow case (Section 3.3).

It is of interest to know whether both Paratethys and the Mediterranean were reconnected to the Indian Ocean in P3. Our model results suggest that an answer could be found comparing paleo-temperature proxies of Paratethys with those of the Mediterranean. The Mediterranean temperature is only sensitive to the gateway connecting the Mediterranean Sea to the Indian Ocean (GMI) and, therefore, opening only GMI can cause the Mediterranean temperature to increase (~3 °C). The Paratethyan temperature, however, is sensitive to both gateways connecting the Indian Ocean to the Paratethys and the Mediterranean (GPI and GMI). Opening either GPI or GMI separately results in approximately the same increase in temperature of Paratethys (~3 °C) while opening both gateways causes a higher increase (~4 °C). It should be noted that we do not have sufficient paleo-temperature data for the Mediterranean to test this scenario.

In the Early Serravallian (13.8–13.4 Ma), a series of geodynamic events affected the Paratethys and the eastern part became isolated from its western counterpart which experienced a severe salinity crisis (de Leeuw et al., 2010). Soon thereafter, however, the whole Paratethys reunited. It is therefore expected to have had a temperature and salinity in line with model predictions for P3, again at the advent of P4.

The final closure of the Indian Ocean gateways (P4) happened during the late Middle Miocene (Rögl, 1999; Meulenkamp and Sissingh, 2003; Popov et al., 2004; Harzhauser et al., 2007a) but its exact timing is not known (Hüsing et al., 2009). As before, we expect closure to have resulted in cooling of the Paratethys (again going from A to B in Fig. 8c and d). Proxy data also show cooling of the Paratethys

in P4 albeit with a different magnitude. The reason for this is that P4 coincides with the period of global climatic deterioration known as the Middle Miocene Climatic Transition (MMCT). We propose that the cooling trend in Paratethys should again be more pronounced than in the global ocean due to gateway closure and disconnection from the warm Indian Ocean. It was also deduced (Section 4.1) that cooling was more pronounced in Paratethys than in the Mediterranean during the Serravallian (Bicchi et al., 2003). Based on our model results, we propose this to be related to the following factors: Paratethys had a lower surface heat flux than the Mediterranean after closure (e.g., Fig. 6), the Mediterranean was already disconnected from the Indian Ocean earlier than Paratethys, or both.

In contrast to the temperature response discussed so far, gateway-induced changes in salinity do depend on the choice for net evaporation. Upon closure, positive net evaporation leads to a significantly higher salinity than the Atlantic value and vice versa. Were it possible to infer past salinity of Paratethys, we could use this to estimate the value of net evaporation.

5. Discussion

5.1. Robustness of model results

Here we discuss the extent to which the results presented in the preceding sections depend on the values assumed for some of the model parameters and on other choices made in setting up the model.

Up to this point, we have used a single value for the hydraulic constant of the gateway between the Mediterranean Sea and Paratethys (GMP; $f_{MP} = 0.1$ Sv). We now investigate the effect of choosing different values for f_{MP} . Note that larger f_{MP} corresponds to a deeper and/or wider GMP and vice versa. We use the setup in Section 3.1.4 with negative net evaporation over Paratethys and positive net evaporation over the Mediterranean. This experiment was chosen since it is similar to the present-day Mediterranean–Black Sea system and in this case we know what to expect for the restricted GMP. We consider the solutions in which the gateway ratios are equal i.e., $r_P = r_M$. Fig. 9 shows the salinity and temperature of Paratethys as a function of the hydraulic constant f_{MP} and the gateway ratio r_P . When r_P is kept constant, increasing f_{MP} causes the salinity and temperature of Paratethys to increase. This is due to the increased inflow from the Mediterranean with higher salinity and temperature. It can be seen that salinity and temperature are nearly constant for $f_{MP} > 0.1$. By decreasing f_{MP} , the salinity and temperature of Paratethys decrease owing to reduced inflow of Mediterranean water and a stronger effect of negative net evaporation. On the other hand, the salinity and temperature of the Mediterranean Sea are not affected significantly by changing f_{MP} (on the order of 0.01 psu and 0.01 °C) because the Mediterranean has a connection with the Atlantic Ocean which suppresses the effect of Paratethys.

We accounted for a single gateway between the Mediterranean and Paratethys. It is pertinent to discuss how our analysis would be affected

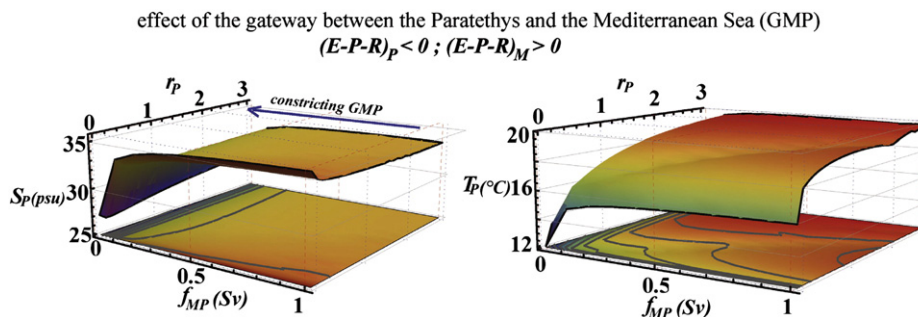


Fig. 9. The salinity and temperature of Paratethys as a function of the hydraulic constant of the gateway between the Mediterranean Sea and Paratethys (f_{MP}) and Paratethys gateway ratio (r_P). Decreasing f_{MP} means constricting the gateway between Paratethys and the Mediterranean Sea (GMP).

if more than one connection were present. Addition of a second gateway between the same two boxes is incompatible with our general setup and different assumptions are needed to determine deep and surface flows in each of the gateways. To the extent that an additional gateway means increasing the connection, we can accommodate such a case simply by increasing the value of hydraulic constant (as was shown in Fig. 9). However, we cannot give details concerning the exchange flow in each of the gateways using a box model. The only way of resolving this issue is to apply an ocean circulation model.

Similarly, we also considered a single value of the hydraulic constant for the connection of the Mediterranean to the Atlantic Ocean ($f_{MA} = 3$ Sv). We have repeated our calculations varying this value between 0.1 and 5 Sv and found that the results do not change significantly.

The Indian Ocean was considered warmer and less saline than the Atlantic Ocean, which we consider the most likely case. However, in the later stage of closure, the seaway connecting the Mediterranean/Paratethys to the Indian Ocean may have had higher salinity than the Indian Ocean itself, as suggested by the occurrence of evaporite deposits in the Mesopotamian basin (Popov et al., 2004). We took the Indian–Ocean box to represent the water properties of this saline seaway by assuming it to be more saline than the Atlantic Ocean and warmer, as before. In this case, although we find an overall increase in salinity of both Paratethys and the Mediterranean prior to closure, the temperature does not change notably. Closure of the Indian Ocean connection, i.e., disconnection from the saline seaway box, leaves both Paratethys and Mediterranean colder as before, but salinity for most cases, depending on net evaporation, will be less than the values prior to closure. Any temperature and salinity difference between the Indian and the Atlantic Ocean can cause salinity and temperature changes in the Mediterranean and Paratethys after closure.

In our box model, the atmospheric forcing was implemented in the form of prescribed, constant, fluxes of freshwater and heat which is a logical first step. This implies that real air–sea interaction is not accounted for and we thus neglect the possibility that changes in water properties feed back to the atmosphere. For example, changes in sea surface temperature could directly influence low level atmospheric temperatures, thereby induce changes in atmospheric circulation and, perhaps, precipitation. The latter would in its turn affect sea surface salinity. In general, understanding the role of air–sea interaction in maintaining the regional climate and the water properties of a basin is a complicated problem which would require an atmosphere–ocean regional climate model with high resolution. There are a few modeling studies for the Mediterranean Sea in which the air–sea interactions were included (e.g., Somot et al., 2008; Artale et al., 2010). According to these authors, the simulation of the Euro-Mediterranean present-day climate does not change significantly by considering the air–sea interactions. Murphy et al. (2009) used an atmosphere model coupled to a slab ocean for the Messinian Mediterranean and asserted that the ocean–atmosphere feedbacks are unlikely to have had an impact on the Mediterranean climate.

For our analysis, we considered the specific case in which the surface and deep flow in the eastern gateways are equal. This may have not been the case in reality. A global scale model analysis (von der Heydt and Dijkstra, 2006) pointed to there being a net westward flow through the Tethys seaway. This means that the ratio of surface to deep flow, which we will refer to as h , does no longer equal unity. In our experiments we find that the net transport decreases when the eastern gateway is restricted. In other words, h decreases in response to a decrease in r_M because of the decrease in the exchange flow with the Indian Ocean. Our calculations show that h is approximately a linear function of r_M , while deep flow is a function of r_M and surface flow is a function of both r_M and r_M^s (see Appendix A). Hence, after some calculation, we can write r_M^s as a function of r_M – as in Section 2.3 – but including a term related to the net flow. Further analysis shows that considering a net flow (surface and deep flows being not equal; $h \neq 1$) does not affect the results. The same

method can be applied to the Paratethys–Indian Ocean gateway. Finally, we point out that our adoption of equal surface and deep flow in the eastern gateways may have suppressed any multiple equilibrium solutions from appearing because it limits the possibilities for the ratio of surface to deep flow. Karami et al. (2009) showed that when multiple solutions exist, the qualitative behavior of each of the solutions in response to closure is similar even though the absolute values are different (in the order of 0.1 psu and 0.1 °C). Moreover, multiple solutions disappeared for closed or restricted gateways to the Indian Ocean. In the present paper, we mainly focus on the changes of salinity and temperature in response to closure and it is not relevant to achieve insight into multiple equilibrium solutions.

5.2. Model-derived insight pertinent to data collection

We found that closure of the gateways to the Indian ocean causes salinity of both Paratethys and Mediterranean to increase if evaporation exceeds precipitation and river discharge in those basins, and vice versa. It follows, that the salinity of an isolated sea is a key predictor to be taken into account in paleoclimatic reconstructions. For instance, we found that upon closure, the salinity of Paratethys is changing from 31 psu to 42 psu (prior to closure is from 32.5 to 36) as we go from negative net evaporation to a positive one. Such changes in Paratethys salinity, in contrast to temperature, cannot easily be attributed to changes in the global ocean and salinity can be used to distinguish between the effects of gateways and climate.

It was shown that the closure of the gateways to the Indian Ocean affects Paratethys and the Mediterranean in a non-linear fashion. This implies that in the advanced stage of the closure, when the gateways to the Indian Ocean are small relative to the other gateways (i.e., $r_M \leq 1$ and $r_P \leq 1$), the changes in temperature and salinity are more significant. On the other hand, the existence of a very shallow and narrow gateway between the Mediterranean Sea and Indian Ocean (e.g., fifty times smaller than the Strait of Gibraltar), or of a small connection between Paratethys and the Indian Ocean (e.g., four times smaller than the Bosphorus) does not have an important influence on the Mediterranean and Paratethys. This would make finding the exact time of closure more complicated, as a very narrow strait to the Indian Ocean could exist but proxies for temperature and salinity will not show it.

5.3. Comparison to previous 3-box model and outlook

Although some of the results presented here were also found with a 3-box model (Karami et al., 2009), e.g., the cooling effect of the Mediterranean Sea/Paratethys, we have obtained more insight into the effect of closure by considering Paratethys as a separate unit. We have also presented new results regarding the changes in water properties of Paratethys and have been able to give an improved presentation of the exchange flows. We can now address the cases with different net evaporation over the Mediterranean and Paratethys and examine role of each of the gateways independently. In terms of the Mediterranean Sea, we found that adding the separate box for Paratethys does not affect the Mediterranean Sea significantly.

Using the 4-box model, we find that prior to closure Paratethys, in contrast to the Mediterranean, is sensitive to changes in net evaporation and heat flux. From this we expect that prior to closure, changes in proxies of the Mediterranean and the global ocean are of the same order, but the changes would be larger for Paratethys. Upon closure, both the Mediterranean and Paratethys are sensitive to climatic changes. These arguments might be helpful to evaluate different opinions regarding the timing of closure. For instance, Allen and Armstrong (2008) suggested that final closure occurred in the late Oligocene. In this case we would expect larger cooling in both the Mediterranean and Paratethys compared with the global ocean already between the Late Oligocene (Late Oligocene warming) and the Early Miocene. This could be

evaluated if temperatures of the Mediterranean Sea and Paratethys were available to be compared with that of the global ocean.

6. Conclusions

We used a 4-box model to study the factors controlling the salinity and temperature of Paratethys and the Mediterranean Sea during the Miocene, when open gateways to the Indian Ocean existed, and in particular the effect of closing these gateways. Because data concerning the atmospheric forcing (net evaporation and heat flux) and paleo-gateways are missing for the Miocene case, we considered a range of values. The evolution of the temperature and salinity of Paratethys and Mediterranean depends heavily on the gateways to the open ocean. We compared our model results to the Miocene history of closure of Paratethys and its proxy data. We have shown that the changes observed in temperature proxies of Paratethys may have been caused by variations of the gateways and do not necessarily reflect climate change. Our results contribute to the understanding of the evolution of semi-enclosed basins. Specific conclusions are the following:

1. Paratethys is more responsive to changes in atmospheric forcing (net evaporation and heat flux) than the Mediterranean Sea when gateways to the Indian Ocean are present. Closure of these gateways increases the sensitivity of Paratethys even more.
2. Under a range of net evaporation scenarios and most values of net surface heat flux, closure results in cooling of Paratethys. The enigmatic mid-Burdigalian cooling observed in the sedimentary record of Paratethys can thus be explained by closure of the gateways between Paratethys/Mediterranean and the Indian Ocean.
3. Closure of the gateways to the Indian Ocean induces a change in salinity of Paratethys which is determined by net evaporation (i.e., the difference between evaporation, precipitation and river discharge) and the size of the gateway connecting Paratethys to the Mediterranean (GMP). Salinity estimations can be used to distinguish between the effects of gateways and climate since changes in the Paratethyan salinity cannot easily be attributed to changes in the salinity of global ocean.
4. Paratethys is responsive to closure of both the gateway between Paratethys and the Indian Ocean (GPI), and the gateway between the Mediterranean Sea and the Indian Ocean (GMI).
5. Paratethys is influenced by the water properties of the Mediterranean Sea. Constriction of the gateway between Paratethys and the Mediterranean Sea (GMP) results in divergence of the water properties of these two basins and may cause cooling of the Paratethys.
6. The Mediterranean Sea is not responsive to closure of the gateway between Paratethys and the Indian Ocean. The water properties of Paratethys have very little influence on the water properties of the Mediterranean Sea.
7. In the advanced stage of the closure, when the gateways to the Indian Ocean were the same size or smaller than the gateway to the Atlantic Ocean (i.e., $r_M \leq 1$ and $r_P \leq 1$), the Mediterranean/Paratethyan temperature and salinity were more responsive to the restriction of the eastern gateways.

Acknowledgments

This research was funded by the Utrecht Centre of Geosciences (UCG). We thank Rachel Flecker for valuable suggestions. We are grateful to P. Grunert and the anonymous reviewer for their constructive reviews.

Appendix A

Derivation of equations

The Miocene Paratethys–Mediterranean system was simplified to a 4-box oceanic model. The boxes correspond to the Atlantic Ocean

(identified with subscript A), the Mediterranean Sea (M), Paratethys (P) and the Indian Ocean (I). We apply linear laws for the temporal variation in the salinity and temperature of Paratethys and the Mediterranean:

$$V_M \frac{dS_M}{dt} = \sum_{i=1}^3 (|q_{Mi}^{in}| S_i - |q_{Mi}^{out}| S_M) \quad (1)$$

$$V_M \frac{dT_M}{dt} = \sum_{i=1}^3 (|q_{Mi}^{in}| T_i - |q_{Mi}^{out}| T_M) + \frac{Q_M}{\rho c} \quad (2)$$

$$V_P \frac{dS_P}{dt} = \sum_{j=1}^2 (|q_{Pj}^{in}| S_j - |q_{Pj}^{out}| S_P) \quad (3)$$

$$V_P \frac{dT_P}{dt} = \sum_{j=1}^2 (|q_{Pj}^{in}| T_j - |q_{Pj}^{out}| T_P) + \frac{Q_P}{\rho c} \quad (4)$$

where V is the volume of the box, S is the salinity, T is the temperature, q is the exchange flow, Q is the total net surface heat flux, and ρ and c are the density and the heat capacity of seawater, respectively. The subscripts i and j refer to any of the basins neighboring the Mediterranean and Paratethys and with which the flow exchange occurs. The superscripts *in* and *out* refer to inflow or outflow, respectively.

We assume that the deep advective flow is a linear function of the density difference between the boxes. Therefore, by applying the linearized equation of state for density, the deep flow between two neighboring basins labeled as “ k ” and “ j ” can be written as

$$q_{kj} = f_{kj} (u_{\beta}^* (S_k - S_j) + 0.19 u_{\alpha}^* (T_j - T_k)) \quad (5)$$

where f is the hydraulic constant of the gateway between the basins and represents the gateway geometry, u_{β}^* and u_{α}^* are unity numbers with dimension psu^{-1} and K^{-1} , respectively, and 0.19 is approximately the ratio of the thermal expansion coefficient to the haline contraction coefficient. S_k, S_j, T_k, T_j are salinity and temperature of the neighboring boxes, respectively. For instance, the deep flow between the Mediterranean Sea and Paratethys will be $q_{MP} = f_{MP} (u_{\beta}^* (S_M - S_P) + 0.19 u_{\alpha}^* (T_P - T_M))$. The same rule applies to the deep flow between the Atlantic Ocean and the Mediterranean (q_{MA}), between the Mediterranean and Indian Ocean (q_{MI}), and between Paratethys and the Indian Ocean (q_{PI}). When q_{kj} is a positive value, the deep flow is considered as an outflow for the box “ k ”, and when it is a negative value, it would be an inflow for the box “ k ”.

Surface flows between the Mediterranean Sea and the Atlantic Ocean (q_{MA}^s) and between the Mediterranean Sea and the Indian Ocean (q_{MI}^s), as well as surface flows between Paratethys and the Indian Ocean (q_{PI}^s) and between Paratethys and the Mediterranean (q_{MP}^s), are calculated using the conservation of mass for the Mediterranean and Paratethys boxes. The surface flows are not equal to the corresponding deep flows and are considered to be in the opposite direction. Therefore, for the Mediterranean Sea and Paratethys we obtain

$$q_{MA} + q_{MI} + q_{MP} + (E - P - R)_M = n_{MA} q_{MA}^s + n_{MI} q_{MI}^s + n_{MP} q_{MP}^s \quad (6)$$

$$q_{PI} + q_{MP} + (E - P - R)_P = n_{PI} q_{PI}^s + n_{MP} q_{MP}^s \quad (7)$$

where n_{kj} is equal to $\text{Sign}(q_{kj})$ and $(E - P - R)$ indicates the net evaporation for the Mediterranean (with subscript M) and Paratethys (with subscript P).

As the objective of this study is to investigate the role of the eastern gateways connecting to the Indian Ocean, we define the exchange flow in the eastern gateway as a function of the exchange flow in the western gateway. For this purpose, we define r_M as the ratio of the hydraulic constant of the eastern gateway of the Mediterranean, to the hydraulic constant of its western gateway. r_P is the equivalent ratio for Paratethys.

As a result, for the deep flow between the Mediterranean Sea and the Indian Ocean, and between Paratethys and the Indian Ocean we obtain

$$\begin{aligned} q_{MI} &= r_M f_{MA} (u_{\beta}^* (S_M - S_I) + 0.19 u_{\alpha}^* (T_I - T_M)) \\ &= r_M f_{MA} u_{\beta}^* ((S_M - S_A - \delta S) + 0.19 u_{\alpha}^* (T_A - T_M + \delta T)) \quad (8) \\ &= r_M q_{MA} - r_M f_{MA} (u_{\beta}^* \delta S - u_{\alpha}^* \delta T) \end{aligned}$$

$$q_{PI} = r_P f_{MP} (u_{\beta}^* (S_P - S_A) + 0.19 u_{\alpha}^* (T_A - T_P) - (u_{\beta}^* \delta S - 0.19 u_{\alpha}^* \delta T)). \quad (9)$$

In addition, we define r_M^s and r_P^s as the ratio of the surface flow in the eastern gateway to surface flow in the western gateway for the Mediterranean and Paratethys, respectively, i.e., $r_M^s = \frac{q_{MI}^s}{q_{MA}^s}$ and $r_P^s = \frac{q_{PI}^s}{q_{MP}^s}$. Thus, from Eqs. (6), (7), (8) and (9) we obtain

$$\begin{aligned} q_{MP}^s &= \frac{1}{-n_{MP} + r_P^s n_{PI}} [-q_{MP} + r_P f_{MP} (u_{\beta}^* (S_P - S_A) + 0.19 u_{\alpha}^* (T_A - T_P)) \\ &\quad - r_P f_{MP} (u_{\beta}^* \delta S - 0.19 u_{\alpha}^* \delta T) + (E - P - R)_P] \quad (10) \end{aligned}$$

$$\begin{aligned} q_{MA}^s &= \frac{1}{n_{MA} + r_M^s n_{MI}} [q_{MA} + r_M q_{MA} - r_M f_{MA} (u_{\beta}^* \delta S - 0.19 u_{\alpha}^* \delta T) \\ &\quad + q_{MP} - n_{MP} q_{MP}^s + (E - P - R)_M] \quad (11) \end{aligned}$$

Now, we solve Eqs. (1)–(5) and Eqs. (8)–(11) for salinity and temperature of the Mediterranean Sea and Paratethys (i.e., S_M , T_M , S_P and T_P). In these equations, f_{MA} , f_{MP} , δS , δT , S_A , T_A , $(E - P - R)$ and Q are the model parameters. We prescribe the value of these parameters based on observations if they exist and if not we try a range of values. The control parameters of the model, which can be used to simulate closure of the gateways to the Indian Ocean, are r_M , r_P , r_M^s and r_P^s and they are not known a priori. As stated in the paper, we try to decrease the number of control parameters by considering two limiting cases. In first case, we assume equal surface and deep flow in the eastern gateways. We use Eqs. (8)–(11) and conditions $q_{PI}^s = q_{PI}$ and $q_{MI}^s = q_{MI}$. This leads us to specific values of r_M^s and r_P^s as a function of r_M , r_P , respectively. Hence, to simulate closure of the surface and deep flow we can use only two parameters (r_M , r_P) instead of four. In second case, we assume a one-layer flow in the gateways to the Indian Ocean which leads to $r_M = 0$ and $r_P = 0$.

References

- Alhammoud, B., Meijer, P.T., Dijkstra, H.A., 2010. Sensitivity of Mediterranean thermohaline circulation to gateway depth: a model investigation. *Paleoceanography* 25, PA2220.
- Allen, M.B., Armstrong, H.A., 2008. Arabia–Eurasia collision and the forcing of mid-Cenozoic global cooling. *Palaeogeography Palaeoclimatology Palaeoecology* 265 (1–2), 52–58.
- Artale, V., Calmanti, S., Carillo, A., Dell'Aquila, A., Herrmann, M., Pisacane, G., Ruti, P.M., Sannino, G., Struglia, M.V., Giorgi, F., Bi, X., Pal, J.S., Rauscher, S., 2010. An atmosphere–ocean regional climate model for the Mediterranean area: assessment of a present climate simulation. *Climate Dynamics* 35, 721–740. doi:10.1007/s00382-009-0691-8.
- Bachmann, A., 1973. Die Silicoflagellaten aus dem Stratotypus des Otnangien. In: Papp, A., Rögl, F., Seneš, J. (Eds.), M2 – Otnangien. Die Innviertler, Salgótarján, Bántapusztaer Schichtengruppe und die Rzehakia Formation: Chronostratigraphie und Neostratypen, Miozän der Zentralen Paratethys, 3, pp. 275–295.
- Baldi, K., 2006. Paleoclimatology and climate of the Badenian (Middle Miocene, 16.4–13.0 Ma) in the Central Paratethys based on foraminifera and stable isotope ($\delta^{18}\text{O}$ and $\delta^{13}\text{C}$) evidence. *International Journal of Earth Sciences* 95, 119–142.
- Bartoli, G., Sarnthein, M., Weinelt, M., Erlenkeuser, H., Garbe-Schonberg, D., Lea, D.W., 2005. Final closure of Panama and the onset of northern hemisphere glaciation. *Earth and Planetary Science Letters* 237 (1–2), 33–44.
- Bicchi, E., Ferrero, E., Goner, M., 2003. Palaeoclimatic interpretation based on Middle Miocene planktonic Foraminifera: the Silesia Basin (Paratethys) and Monferrato (Tethys) records. *Palaeogeography Palaeoclimatology Palaeoecology* 196, 265–303.
- Bohn-Havas, M., Zorn, I., 2003. Planktonic gastropods (pteropods) from the Karpatian of the Central Paratethys. In: Brzobohatý, R., Cicha, I., Kováč, M., Rögl, F. (Eds.), The Karpatian—A Lower Miocene Stage of the Central Paratethys. Masaryk University, Brno, pp. 203–211.

- Brzobohatý, R., Nolf, D., Kroupa, O., 2007. Fish otoliths from the Middle Miocene of Kienberg at Mikulov, Czech Republic, Vienna Basin: their paleoenvironmental and paleogeographic significance. *Bulletin de l'Institut royal des Sciences naturelles de Belgique, Sci. Terre, Bruxelles, Institut roy. des sci. nat. de Belgique* 77, 167–196.
- Burns, D.A., Nelson, C.S., 1981. Oxygen isotopic paleotemperatures across the Runangan–Whaingaroan (Eocene–Oligocene) boundary in a New Zealand shelf sequence. *New Zealand Journal of Geology and Geophysics* 24, 529–538.
- Cicha, I., Rögl, F., Rupp, C., Čtyroká, J., 1998. Oligocene–Miocene foraminifera of the Central Paratethys. *Abhandlungen Senckenberg Naturforschende Gesell* 549, 1–325.
- Cicha, I., Rögl, F., Čtyroká, J., 2003. Central Paratethys Karpatian foraminifera. In: Brzobohatý, R., Cicha, I., Kováč, M., Rögl, F. (Eds.), The Karpatian—An Early Miocene Stage of the Central Paratethys. Masaryk University, Brno, pp. 169–188.
- Čorić, S., Harzhauser, M., Hohenegger, J., Mandić, O., Pervesler, P., Roetzel, R., Rögl, F., Scholger, R., Spezzaferri, S., Stingl, K., Švábenická, L., Zorn, I., Zuschin, M., 2004. Stratigraphy and correlation of the Grund Formation in the Molasse Basin, northeastern Austria (Middle Miocene, Lower Badenian). *Geol Carpathica* 55 (2), 207–215.
- Dumitrică, P., Ghe, N., Popescu, Gh., 1975. New data of the biostratigraphy and correlation of the Middle Miocene in the Carpathian Area, LXI/4. *Dări de Seamă I.G.G. Bucuresti*, pp. 65–84 (1973–1974).
- De Leeuw, A., Bukowski, K., Krijgsman, W., Kuiper, K.F., 2010. Age of the Badenian salinity crisis: impact of Miocene climate variability on the circum Mediterranean region. *Geology* 38 (8), 715–718.
- Filipescu, S., 2001. The Miocene from the western border of the Transylvanian Depression. In: Bucur, I.L., Filipescu, S., Sasaran, E. (Eds.), *Algae and Carbonate Platforms in Western Part of Romania*. 4th Regional Meeting of IFAA Cluj-Napoca 2001, Field Trip Guidebook, pp. 109–118.
- Goner, M., Peryt, T.M., Durakiewicz, T., 2000. Biostratigraphical and palaeoenvironmental implications of isotopic studies ($\delta^{18}\text{O}$, $\delta^{13}\text{C}$) of middle Miocene (Badenian) foraminifera in the Central Paratethys. *Terra Nova* 12, 231–238.
- Grunert, P., Soliman, A., Harzhauser, M., Müllberger, S., Piller, W.E., Rögl, F., 2010. Upwelling conditions in the Early Miocene Central Paratethys Sea. *Geologica Carpathica* 61 (2), 129–145.
- Hall, C.A., 1964. Shallow-water marine climates and molluscan provinces. *Ecology* 45 (2), 226–234. doi:10.2307/1933835.
- Harzhauser, M., 2002. Marine und brachyhaline Gastropoden aus dem Karpatium des Korneuburger Beckens und der Kreuzstettner Bucht (Österreich, Untermiozän). *Beiträge zur Paläontologie* 27, 61–159.
- Harzhauser, M., 2003. The marine gastropods, scaphopods and cephalopods of the Karpatian in the central Paratethys. In: Brzobohatý, R., Cicha, I., Kováč, M., Rögl, F. (Eds.), The Karpatian—An Early Miocene Stage of the Central Paratethys. Masaryk University, Brno, pp. 193–202.
- Harzhauser, M., Piller, W.E., 2007. Benchmark data of a changing sea—Palaeogeography, Palaeobiogeography and events in the Central Paratethys during the Miocene. *Palaeogeography Palaeoclimatology Palaeoecology* 253, 8–31.
- Harzhauser, M., Piller, W.E., Steininger, F.F., 2002. Circum-Mediterranean Oligo-Miocene biogeographic evolution—the gastropods' point of view. *Palaeogeography Palaeoclimatology Palaeoecology* 183 (1–2), 103–133.
- Harzhauser, M., Mandić, O., Zuschin, M., 2003. Changes in Paratethyan marine molluscs at the Early/Middle Miocene transition—diversity, paleogeography and paleoclimate. *Acta Geol Pol* 53, 323–339.
- Harzhauser, M., Kroh, A., Mandić, O., Piller, W.E., Göhlich, U., Reuter, M., Berning, B., 2007a. Biogeographic responses to geodynamics: a key study all around the Oligo-Miocene Tethyan Seaway. *Zoologischer Anzeiger A Journal of Comparative Zoology* 246 (4), 241–256.
- Harzhauser, M., Piller, W.E., Latal, C., 2007b. Geodynamic impact on the stable isotope signatures in a shallow epicontinental sea. *Terra Nova* 19, 324–330.
- Haug, G.H., Tiedemann, R., 1998. Effect of the formation of the isthmus of Panama on Atlantic Ocean thermohaline circulation. *Nature* 393, 673–676.
- Hay, W.W., 1996. Tectonics and climate. *Geologische Rundschau* 85, 409–437.
- Hilgen, F.J., Abels, H.A., Iaccarino, S., Krijgsman, W., Raffi, I., Sprovieri, R., Turco, E., Zachariasse, W.J., 2009. The Global Stratotype Section and Point (GSSP) of the Serravallian Stage (Middle Miocene). *Episodes* 32, 152–166.
- Hopkins, T.S., 1999. The thermohaline forcing of the Gibraltar exchange. *Journal of Marine Systems* 20 (1–4), 1–31.
- Hüsing, S.K., Zachariasse, W.J., Van Hinsbergen, D.J.J., Krijgsman, W., Inceöz, M., Harzhauser, M., Mandić, O., Kroh, A., 2009. Oligo-Miocene foreland basin evolution in SE Anatolia: implications for the closure of the eastern Tethys gateway. In: Van Hinsbergen, D.J.J., Edwards, M.A., Govers, R. (Eds.), *Geodynamics of Collision and Collapse at the Africa–Arabia–Eurasia Subduction Zone*: Geological Society of London Special Publication, 311, pp. 107–132.
- Jiříček, R., 1983. Redefinition of the Oligocene and Neogene ostracod zonation of the Paratethys. I. *Knihovnička ZPN, Miscell, Micropal*, pp. 195–236.
- Kamp, P.J., Waghorn, D.B., Nelson, C.S., 1990. Late eocene–early oligocene integrated isotope stratigraphy and biostratigraphy for paleoshelf sequences in southern Australia: paleoceanographic implications. *Palaeogeography Palaeoclimatology Palaeoecology* 80, 311–323. doi:10.1016/0031-0182(90)90140-3.
- Kara, A.B., Wallcraft, A.J., Hurlburt, H.E., Stanev, E.V., 2008. Air–sea fluxes and river discharges in the Black Sea with a focus on the Danube and Bosphorus. *Journal of Marine Systems* 74 (1–2), 74–95.
- Karami, M.P., Meijer, P.T., Dijkstra, H.A., Wortel, M.J.R., 2009. An oceanic box model of the Miocene Mediterranean Sea with emphasis on the effects of closure of the eastern gateway. *Paleoceanography* 24, PA4203.
- Kocsis, L., Venemann, T.W., Fontignie, D., Baumgartner, C., Montanari, A., Jelen, B., 2008. Oceanographic and climatic evolution of the Miocene Mediterranean deduced from Nd, Sr, C, and O isotope compositions of marine fossils and sediments. *Paleoceanography* 23, PA4211.

- Kováč, M., Andreyev, A., Grigorovich, A., Bajraktarević, Z., Brzobohatý, R., Filipescu, S., Fodor, L., Harzhauser, M., Nagymarosy, A., Oszczypko, N., Pavelić, D., Rögl, F., Saftić, B., Sliva, L., Studencka, B., 2007. Badenian evolution of the Central Paratethys Sea: paleogeography, climate and eustatic sea-level changes. *Geologica Carpathica* 58 (6), 579–606.
- Kroh, A., 2003. Echinoderms of the Karpatian. In: Brzobohatý, R., Cicha, I., Kováč, M., Rögl, F. (Eds.), *The Karpatian—A Lower Miocene Stage of the Central Paratethys*. Masaryk University, Brno, pp. 247–256.
- Kroh, A., 2007. Climate changes in the Early to Middle Miocene of the Central Paratethys and the origin of its echinoderm fauna. *Palaeogeography Palaeoclimatology Palaeoecology* 253 (1–2), 169–207.
- Latal, C., Piller, W.E., Harzhauser, M., 2004. Palaeoenvironmental reconstructions by stable isotopes of Middle Miocene gastropods of the Central Paratethys. *Palaeogeography Palaeoclimatology Palaeoecology* 211 (1–2), 157–169.
- Latal, C., Piller, W.E., Harzhauser, M., 2006. Shifts in oxygen and carbon isotope signals in marine mollusks from the Central Paratethys (Europe) around the Lower/Middle Miocene transition. *Palaeogeography Palaeoclimatology Palaeoecology* 231, 347–360.
- Mandic, O., 2003. Bivalves of the Karpatian in the Central Paratethys. In: Brzobohatý, R., Cicha, I., Kováč, M., Rögl, F. (Eds.), *The Karpatian—A Lower Miocene Stage of the Central Paratethys*. Masaryk University, Brno, pp. 217–227.
- Mandic, O., Steininger, F.F., 2003. Computer-based mollusc stratigraphy—a case study from the Eggenburgian (Early Miocene) type region (NE Austria)—Palaeogeography. *Palaeoclimatology Palaeoecology* 197, 263–291.
- Mandic, O., Harzhauser, M., Roetzel, R., 2004. Taphonomy of spectacular shell accumulations from the type stratum of the Central Paratethys stage Eggenburgian (Early Miocene, NE Austria). *Courier Forschungsinstitut Senckenberg* 246, 69–88.
- Meijer, P.Th., 2006. A box model of blocked-outflow scenario for the Messinian salinity crisis. *Earth and Planetary Science Letters* 248, 486–494.
- Meulenkamp, J.E., Sissingh, W., 2003. Tertiary palaeogeography and tectonostratigraphic evolution of the Northern and Southern Peri-Tethys platforms and the intermediate domains of the African–Eurasian convergent plate boundary zone. *Palaeogeography Palaeoclimatology Palaeoecology* 196, 209–228.
- Murphy, L.N., Kirk-Davidoff, D.B., Mahowald, N., Otto-Bliesner, B.L., 2009. A numerical study of the climate response to lowered Mediterranean sea level during the Messinian salinity crisis. *Palaeogeography Palaeoclimatology Palaeoecology* 279 (1–2), 41–59.
- Nebelsick, J.H., 1989. Temperate water carbonate facies of the Early Miocene Paratethys (Zogelsdorf Formation, Lower Austria). *Facies* 21, 11–40.
- Ogasawara, K., 1994. Neogene paleogeography and marine climate of the Japanese Islands based on shallow-marine mollusks. *Palaeogeography Palaeoclimatology Palaeoecology* 108, 335–351. doi:10.1016/0031-0182(94)90241-0.
- Omta, A.W., Dijkstra, H.A., 2003. A physical mechanism for the Atlantic–Pacific flow reversal in the early Miocene. *Global and Planetary Change* 36 (4), 265–276.
- Piller, W.E., Harzhauser, M., Mandic, O., 2007. Miocene Central Paratethys stratigraphy—current status and future directions. *Stratigraphy* 4, 151–168.
- Pocknall, D.T., 1990. Palynological evidence for the early to middle Eocene vegetation and climate history of New Zealand. *Review of Palaeobotany and Palynology* 65, 57–69.
- Popov, S.V., Rögl, F., Rozanov, A., 2004. Lithological-paleogeographic maps of Paratethys: 10 maps Late Eocene to Pliocene. *Courier Forschungsinstitut Senckenberg* 250, 1–46.
- Ramstein, G., Fluteau, F., Besse, J., Joussaume, S., 1997. Effect of orogeny, plate motion and land–sea distribution on Eurasian climate change over the past 30 million years. *Nature* 386, 788–795.
- Reichenbacher, B., 1998. Fisch-Otolithen aus dem Karpat des Korneuburger Beckens. *Beiträge zur Paläontologie* 23, 325–345.
- Reuter, M., Piller, W.E., Harzhauser, M., Mandic, O., Berning, B., Rögl, F., Kroh, A., Aubry, M.P., Wielandt-Schuster, U., Hamedani, A., 2009. The Oligo-/Miocene Qom Formation (Iran): evidence for an early Burdigalian restriction of the Tethyan Seaway and closure of its Iranian gateways. *International Journal of Earth Sciences* 98, 627–650.
- Rögl, F., 1998. Palaeogeographic considerations for Mediterranean and Paratethys seaways (Oligocene to Miocene). *Annalen des Naturhistorischen Museums in Wien* 99, 279–310.
- Rögl, F., 1999. Mediterranean and Paratethys. Facts and hypotheses of an Oligocene to Miocene paleogeography (short overview). *Geologica Carpathica* 50 (4), 339–349.
- Rögl, F., Brzobohatý, R., Cicha, I., Coric, S., Daxner-Höck, G., Dolakova, N., Harzhauser, M., 2003. Paleobiological characterization and definition of the Karpatian stage. In: Brzobohatý, R., Cicha, I., Kováč, M., Rögl, F. (Eds.), *The Karpatian—A Lower Miocene Stage of the Central Paratethys*. Masaryk University, Brno, pp. 357–360.
- Schultz, O., 1998. Die Knorpel- und Knochenfischfauna (excl. Otolithen) aus dem Karpat des Korneuburger Beckens (Niederösterreich). *Beiträge zur Paläontologie* 23, 295–323.
- Schultz, O., 2003. The middle Miocene fish fauna (excl. Otoliths) from Muhlbach am Manhartsberg and Grund near Hollabrunn, Lower Austria. *Annalen des Naturhistorischen Museums in Wien* 104A, 185–193.
- Somot, S., Sevault, F., Déqué, M., Crépon, M., 2008. 21st century climate change scenario for the Mediterranean using a coupled atmosphere–ocean regional climate model. *Global and Planetary Change* 63, 112–126.
- Spezzaferri, S., Rögl, F., Corić, S., Hohenegger, H., 2004. Paleoenvironmental changes and agglutinated foraminifera across the Karpatian/Badenian (Early/Middle Miocene) boundary in the Styrian Basin (Austria, Central Paratethys). In: Bubik, M., Kaminski, M.A. (Eds.), *Proceedings of the Sixth International Workshop on Agglutinated Foraminifera*. Grzybowski Foundation: Spec. Publ., 8, pp. 423–459.
- Stewart, D.R.M., Pearson, P.N., Ditchfield, P.W., Singano, J.M., 2004. Miocene tropical Indian Ocean temperatures: evidence from three exceptionally preserved foraminiferal assemblages from Tanzania. *Journal of African Earth Sciences* 40 (3–4), 173–189.
- Stommel, H., 1961. Thermohaline convection with two stable regimes of flow. *Tellus* 13, 224–230.
- Studencka, B., Gontsharova, I.A., Popov, S.V., 1998. The bivalve faunas as a basis for reconstruction of the Middle Miocene history of the Paratethys. *Acta Geol Pol* 48 (3), 285–342.
- Thompson, B., Nilsson, J., Nycander, J., Jakobsson, M., Döös, K., 2010. Ventilation of the Miocene Arctic Ocean: an idealized model study. *Paleoceanography* 25, PA4216. doi:10.1029/2009PA001883.
- Toth, E., Gorog, A., Lecuyer, C., Moissette, P., Balter, V., Monostori, M., 2010. Palaeoenvironmental reconstruction of the Sarmatian (Middle Miocene) Central Paratethys based on palaeontological and geochemical analyses of foraminifera, ostracods, gastropods and rodents. *Geological Magazine* 147 (2), 299–314.
- Von der Heydt, A., Dijkstra, H.A., 2005. Flow reorganizations in the Panama Seaway: a cause for the demise of Miocene corals? *Geophysical Research Letters* 32, L02609.
- Von der Heydt, A., Dijkstra, H.A., 2006. Effect of ocean gateways on the global ocean circulation in the late Oligocene and early Miocene. *Paleoceanography* 21, PA1011.
- Zachos, J.C., Dickens, G.R., Zeebe, R.E., 2008. An early Cenozoic perspective on greenhouse warming and carbon-cycle dynamics. *Nature* 451, 279–283. doi:10.1038/nature06588.
- Zhang, Z., Wang, H., Guo, Z., Jiang, D., 2007. What triggers the transition of palaeoenvironmental patterns in China, the Tibetan Plateau uplift or the Paratethys Sea retreat. *Palaeogeography Palaeoclimatology Palaeoecology* 245, 317–331.